ADAPTATION OF A CLINICAL MULTIPARAMETER FLOW CYTOMETRY STRATEGY FOR THE ENRICHMENT OF MEASURABLE RESIDUAL DISEASE CELLS IN ACUTE MYELOID LEUKEMIA

ADAPTATION OF A CLINICAL MULTIPARAMETER FLOW CYTOMETRY STRATEGY FOR THE ENRICHMENT OF MEASURABLE RESIDUAL DISEASE CELLS IN ACUTE MYELOID LEUKEMIA

BY SARA PISHYAR, HBSC

Thesis Submitted to the School of Graduate Studies in Partial Fulfilment of the Requirements for the Degree Master of Science

McMaster University

McMaster University MASTER OF SCIENCE (2022) Hamilton, Ontario
(Biochemistry and Biomedical Sciences)

TITLE: Prospective Isolation and Characterization of Measurable Residual Disease in Acute Myeloid Leukemia.

AUTHOR: Sara Pishyar, HBSc.(McMaster University).

SUPERVISOR: Dr. Tobias Berg.

NUMBER OF PAGES: X, 60

Lay Abstract

Acute Myeloid Leukemia (AML) is a type of blood cancer originating in the bone marrow. Even after intense treatment, only 40-50% of AML patients maintain complete remission and the majority of AML patients will unfortunately experience an aggressive relapse. Measurable residual disease (MRD) cells are cells that remain in patients post-treatment. Our research goal is to understand the biology of these MRD cells better. We therefore aim to enrich MRD cells to study them at a molecular level to understand how they could be better targeted for future treatments. Our research may therefore aid in patient prognosis, development of personalized treatment, and reduction of relapse.

Abstract

Acute myeloid leukemia (AML) is a heterogenous blood cancer originating in the bone marrow and arising from the abnormal growth and lack of differentiation of myeloid cells. Even after intense treatment, disease recurrence is a major problem in AML and is attributed to cells that remain following treatment. We are now able to detect these residual cells after treatment with sensitive assays. This is known as measurable residual disease cells (MRD).

The detection of MRD is possible using multiparameter flow cytometry assays and quantitative PCR (qPCR). The detection of MRD has been shown to be predictive of survival. However, there is very limited understanding of the biology of MRD as it is currently not possible to isolate MRD cells and study them in functional assay or by gene expression assays.

Our research now aimed to modify methods used for MRD detection to allow for the isolation and characterization of MRD cells from remission samples. To facilitate this, a recently published a multiparameter flow cytometry (MFC) panel based on the ELN recommendations was established and modified for use on frozen samples. This panel allows to the identification of early myeloid progenitor cells and the asynchronous expression of maturation markers as well as the aberrant expression of lineage markers. To identify patient samples with MRD, we used sensitive clinical qPCR assays for the detection of different NPM1 mutations as well as RUNX1-RUNX1T1. More than 160 samples from 86 patients were collected and samples with MRD identified from 3 patients. Based on our MFC panel we sorted these cells from the follow up samples through the use of either early myeloid progenitor markers, or aberrant marker expression. Using this approach, we could enrich for the level of MRD in these samples. This method is now available and could be a first step in the prospective isolation of MRD cells for functional studies and gene expression profiling.

Acknowledgments

I would like to thank my supervisor, Dr. Tobias Berg for his guidance, as well as his contagious dedication and passion for research. He has been a role model, not just as a clinician and a researcher, but as a true leader. His continuous support has helped shape me into a scientist; curious, patient, and self-reliant. I would also like to extend my thanks to the committee members; Dr. Brian Leber, Dr. Clinton Campbell, and Dr. Mick Bhatia. As well, I would like to thank Dr. Kanwaldeep Singh for his help throughout this degree. He has been supportive, encouraging and his assistance is greatly appreciated by the Berg lab. This research could not have been made possible without the aid of healthcare professionals at Juravinski Hospital. I would like to finally thank the Berg lab members, especially my best friend Pradhariny Prabagaran.

List of Abbreviations

ARA-C	Cytarabine
ALL	Acute lymphoid leukemia
AML	Acute myeloid leukemia
APL	Acute promyelocytic leukemia
CH	Clonal hematopoesis
CLL	Chronic lymphoid leukemia
CML	Chronic myeloid leukemia
CR	Complete remission
DNMT3	DNA methyl transferase
DTA	DNMT31, TET2, ASXL1
FAB	French, American, British
FACS	Fluorescence active cell sorter
FMO	Fluorescence minus one
HSCT	Hematopoietic stem cell transplant
ITD	Internal tandem repeat
LAIP	Leukemia associated immunophenotype
MFC	Multiparameter flow cytometry
MPM	Myeloid progenitor marker(s)
MRD	Measurable residual disease
NPM1	Neucleophosmin 1
PEF	PBS, EDTA, FBS
PMT	Photomultiplier tube
qPCR	Quantitative PCR
sCR	Stringent complete remission

List of Figures and Tables

Chapter 1: Introduction

1.1 Leukemia Classification

Leukemias are blood cancers originating in the bone marrow and can affect people of all ages. These diseases arise due to a variety of factors, both environmental and genetic. Clinically, leukemia is classified based on the type of blood cell affected, and the rate of disease progression. While chronic leukemias are characterized by an increase in differentiated cells, acute leukemias are characterized by an accumulation of immature and non-functional cells which then also impairs the formation of normal blood cells (Leukemia, 2018).

The majority of leukemias can be classified as Acute Myeloid Leukemia (AML), Acute Lymphoid Leukemia (ALL), Chronic Myeloid Leukemia (CML), and Chronic Lymphoid Leukemia (CLL). For most individuals suffering from these diseases, it can be classified by one of these subgroups. In patients with acute myeloid leukemia, cells resembling early myeloid progenitors accumulate (myeloblasts, typically called blasts). Blasts are immature cells that accumulate in the bone marrow and other organs, which inhibits the formation of normal blood cells and can cause infections and bleeding if left untreated. In patients diagnosed with lymphoid leukemias typically exhibit overproduction and aberrant differentiation of the multipotent lymphoid progenitor. AML is characteristically defined by a blast count more than 20% blasts in the bone marrow (Gilliland & Tallman, 2002). This disease is the focus of our work.

AML arises on the background of the hematopoietic system by the acquisition of mutations. The hematopoietic system is organized as a hierarchy with hematopoietic stem cells at the apex. These give rise to multipotent myeloid progenitors, and multipotent lymphoid progenitors (Figure 1).

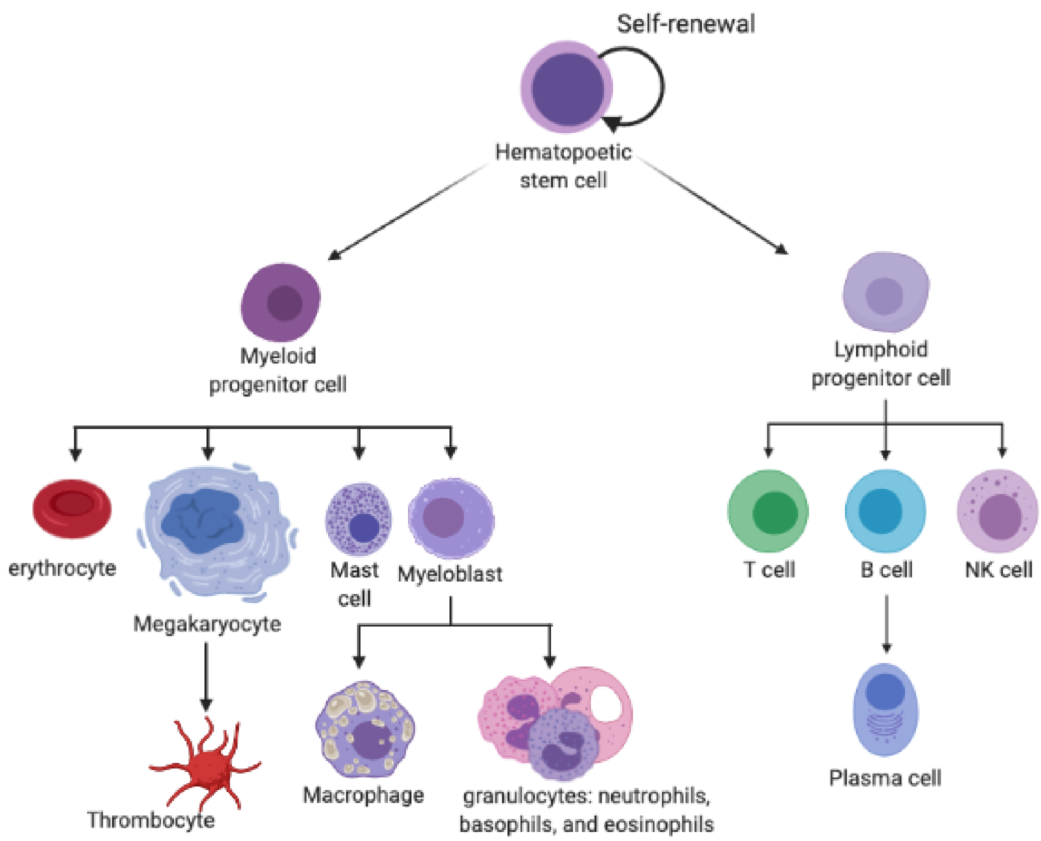

Figure 1. Simplified diagram of hematopoiesis. Diagram illustrates HSCs at the apex followed by the progenitor cells. This diagram represents normal patterns of differentiation.

1.1.1 Epidemiology and etiology of AML

In 2020, approximately 7000 Canadians were diagnosed with leukemia, and 3000 Canadians have died from this disease according to Canadian Cancer Statistics (leukemia statistics, 2020). The age at which AML patients are diagnosed is typically around 65-74, however, younger individuals can also be diagnosed with this disease (Facts and Statistics: Blood Cancer, 2016). While the disease can be treated, most patients will relapse within 3 years and the 5 year OS for patients with AML (>20 years of age) is 27% (Siegel RL, 2022) (Estey & Dohner , 2006).The disease is characterized by a great heterogeneity. There are numerous chromosomal and molecular abnormalities found, many of which are recurrent and therefore believed to drive leukemogenesis. For instance, cytogenetic abnormalities are found in approximately 50-60% of AML cases, of which the majority of patients have monosomies and trisomies on chromosome 5, 7 and 8. Other common chromosomal abnormalities are translocations such as the translocation t(8;21), t(15;17), inversion of chromosome 16 (inv16) (Martens JHA., 2010).The chromosomal translocations lead to the formation of fusion proteins that often involve essential myeloid transcription factors and alter the expression of genes necessary for normal development of myeloid cells (Mitelman F, 2007).

Identification of mutations in transcription factors or other factors, such as tyrosine kinases, has led to a classification of mutations into two classes: class I comprises of mutations which increase the proliferation of progenitor cells, while class II mutations are able to reduce differentiation and often intensify self-renewal (Gilliland DG., 2002). This model is called the two-hit hypothesis model designed to showcase the importance of the interaction of a variety of genetic abnormalities. While the two-hit model can explain some of the interactions of mutations found, further characterization of AML using next generation sequencing has shown that in almost all cases of AML more than two hits are required and that often other factors such as factors influencing epigenetic regulation and other fundamental cellular processes for differentiation are affected. The heterogeneity of AML should not be understated; in a large cohort study (1540 patients), 5234 driver mutations have been identified, with 86% of patients presenting 2 or more driver mutations in a large cohort study (1540 patients) (Papaemmanuil, et al., 2016).

The recognition that different underlying mutations and clinical history can lead to large differences in the biology and prognosis of the disease, has led to the integration of these characteristics into the classification of the disease such as the 2016 edition of the WHO classification (Table 1). The individual mutations present in patients also determine the patient prognosis (favourable or adverse); therefore each AML patient will respond to treatment differently, underscoring the importance of individualized treatment.

Table 1. Acute myeloid leukemia classifications adapted from 2016 revision of World Health Organization (Arber, et al., 2019). *The classification includes six AML categories, for our purposes, only 5 are presented. Only a few examples are presented in this table, highlighting the heterogeneity seen in AML.*

MDS: myelodysplasia, AML: Acute myeloid leukemia, NPM1: Nucleophosmin1, NOS: Not otherwise specified

WHO Classifications	Examples
AML with recurrent genetic abnormalities	- AML with t(8;21)(q22;q22.1);RUNX1-RUNX1T1 - AML with inv(16)(p13.1q22) or t(16;16)(p13.1;q22);CBFB-MYH11 - APL with PML_RARA - AML with t(9;11)(p21.3;q23.3); MLLT3-KMT2A - AML with t(6;9)(p23;q34.1));DEK-NUP214 - AML with inv(3)(q21.3126.2) or t(3;3)(q21.3;q26.2);GATA2, MECOM - AML(megakaryoblastic) with t(1;22)(p13.3;q13.3);RBM15-MKL1 - Provisional entity: AML with BCR-ABL1 - AML with mutated NPM1 - AML with biallelic mutations of CEBPA - Provisional entity: AML with mutated RUNX1
AML, NOS	- AML with minimal differentiation - AML without maturation - AML with maturation - Acute myelomonocytic leukemia - Acute monoblastic/monocytic leukemia - Pure erythroid leukemia (Estey & Dohner, 2006) - Acute megakaryoblastic leukemia - Acute basophilic leukemia - Acute panmyelosis with myelofibrosis - AML with Myelodysplasia-related changes - Related to chemotherapy, radiation therapy, immunosuppressive therapy or combinations.
Myeloid proliferations related to Down syndrome	Transient abnormal myelopoiesis (TAM) Myeloid leukemia associated with Down syndrome

1.1.2 Common AML Mutations: NPM1

The WHO classification of AML recognizes AML with mutated nucleophosmin1 (NPM1) as its own entity due to its significant prognostic value, biologic stability, and its commonality as this subgroup constitutes 27% of patients in large cohort studies (Arber, et al., 2019) (Papaemmanuil, et al., 2016). The NPM1 gene is found on chromosome 5. Wildtype NPM1 is involved in numerous processes such as cell proliferation, chaperoning proteins, and involved in stability and transcriptional activity of p53 (Colombo E, 2002). Most NPM1 mutations belong to one of 3 types: accounting for 75% of all NPM1-mutations, NPM1 type A is a duplication of TCTG at the position 863 (860_863dupTCTG). Type B (863_864insCATG) and D (863_864insCCTG) constitute 15% of NPM1-mutations, and the final 10% are infrequent, often patient specific insertions (Suzuki, et al., 2005) (Alpermann, et al., 2016). The most common collaborating mutations found in patients with NPM1 mutations affect FLT3 with internal tandem duplication (ITD) or in the tyrosine kinase domain (TKD) (Daver, Schlenk, Levis, & Russel, 2019). The presence of NPM1-mutation in younger AML patients (<65 years) was associated with a higher overall survival if NPM1-mutation occurred without FLT3-ITD. Work by Krönke et al has shown that NPM1 mutation levels after chemotherapy still impacted overall OS and incidence of relapse (Krönke J, 2011). Another interesting implication arises when Krönke et al identified NPM1 mutation in diagnosis leukemia cells as well as relapsed cells, thus concluding that there is high stability in the presence of NPM1-mutations (Kronke, et al., 2013). This stability of the mutation over time makes NPM1 mutations an excellent target for MRD detection and it is a strong predictor of overall survival (Buccisano F, 2012) (Schuurhuis G, 2018).

1.2 Current treatments

AML treatment is usually started upon diagnosis of the disease. The goal is to achieve complete remission, which means to reduce leukemic blasts in the patient's bone marrow to less than 5% of the cells, which will then allow the normal hematopoiesis to recover. This is done using initial chemotherapy regimens termed induction therapy in which most patients less than 60 years old receive two chemotherapy drugs; cytarabine (Ara-C) and an anthracycline (ex. Daunorubicin). The combination of these two drugs is usually termed 7+3 regimen because seven days of Ara-C and three days of an anthracycline is administered (Dohner, et al., 2017). In addition to Ara-C and an anthracycline, patients can receive other drugs targeting specific factors or cell surface markers unique to their disease. For example, gemtuzumab ozogamicin, an antibody-drug conjugate recognizing human CD33-expressing tumour cells, has been used in conjunction with the 7+3 regimen to improve event-free survival (Hui G, 2020)

To successfully treat aging patients, one must consider the patient's current condition and disease characteristics (Cytogenetic, risk group, etc). As such, high intensity chemotherapy may not be as beneficial to an older patient (65+) (Almeidaa & Fernando, 2016). Low-dose cytarabine and azacytidine are the few treatment regimens for elderly AML patients (Tilly, et al., 1990). The latter drug has been shown to provide elderly patients with a superior OS (Dombret, et al., 2015). The combination of Venetoclax with azacytidine (Vidaza) further improved the OS in older patients (DiNardo, et al., 2020). Once the patient's blast cells have decreased (<5%) and recovered blood counts have reached the appropriate levels (Neutrophil ≥1000/uL, platelets ≥100,000/uL) (Cheson BD, 2003), the patient is now considered to be in a complete remission (CR), and post-remission treatment (consolidation) will be used (Dohner, et al., 2017). If there are residual leukemia cell populations after induction, the AML is considered refractory.

In younger patients, consolidation can include further rounds of high dose cytarabine and/or allogeneic stem cell transplant (allo-SCT). Hematopoietic stem cell transplant (HSCT) is typically administered to patients in intermediate or high- risk group. Older patients with favorable risk groups will respond well to consolidation chemotherapy and for most of them allo-HSCT may not be needed. It is important to note that although there is increasing evidence for usage of allo-HSCT in fit older patients, only about 6% receive transplant (Devine, et al., 2015). This can be due to the physician's reluctancy to select these patients for transplant (Ustun, Lazarus, & Weisdorf, 2013). There are currently a variety of treatments being developed, which have the potential to aid elderly patients to achieve complete remission. For example, with the advances of low-intensive chemotherapy, select older AML patients are now able to receive HSCT safely.

The OS of adult AML patients treated with cytarabine, daunorubicin and HSCT (gold standard) is only 40-50% (Löwenberg B., 2011). This grim statistic has placed pressure on the research community to continue to study AML to identify mechanisms of relapse, and novel targets. Investigating measurable residual disease (MRD) is a relatively new area of research which can potentially aid clinicians to better understand patient prognosis, aid in early intervention, and help identify therapeutic targets for individualized treatments.

1.3 Methods of MRD detection

MRD detection is an important tool for evaluating different approaches to establishing a complete remission in patients with AML. It can also enhance the ability to intervene early in the disease and identifying potential therapeutic targets. Many studies have demonstrated that the presence of MRD (MRD positive) dictated a poor outcome for patients, regardless of patient risk-group. MRD positive patients had lower OS and progression-free survival (Munshi, et al., 2018).

Disease persistence by morphology or cytogenetics after induction can predict a poor prognosis, however even patients achieving a remission may relapse. Assessing MRD can help identify patients with an increased risk of relapse. In one study, patients with less than 10^{-4} of a leukemia-associated immunophenotypes by flow cytometry identified using flow cytometry as good prognosis patients with a low relapse rate. Contrarily, those with MRD greater than 10^{-2} were identified as poor prognosis, and 80% of this adverse group relapsed within 3 years. Interestingly, even patients in favourable cytogenetic groups (t(15;17), t(8;21), inv 16)) who had MRD values greater than 10^{-2} often relapsed, and those with unfavourable cytogenetics (complex, −7, abnormalities in 3q, del (5q) and −5) with MRD values less than 10^{-4} did not relapse (San Miguel, et al., 2001). As well, the persistent detection of MRD by quantitative PCR (qPCR) in NPM1 mutated patients identified those with poor prognosis, with 82% relapse within 3 years (Ivey, et al., 2016).

To help intervene early and establish greater overall survival in patients, it is therefore important to identify MRD positive patients.

MRD detection can be facilitated either by detecting surface markers of AML cells by flow cytometry (MFC) or by quantifying the presence of a specific mutation found in AML, either by quantitative PCR based methods or by the next-generation sequencing. MFC, and qPCR are the two most used methods of MRD detection in clinical settings. The use of flow cytometry and qPCR where possible can facilitate the detection of MRD in a high fraction of patients. I will now introduce these methods.

1.3.1 Quantitative PCR

QPCR, also known as real-time PCR, provides information regarding the abundance of a target DNA sequence. It is for example used to obtain information regarding the relative level of gene activation through means of messenger RNA (mRNA) expression. Transcription explains the steps taken for DNA to be read and transcribed into mRNA. For the purpose of qPCR, mRNA of a specific gene is converted to complementary DNA (cDNA), and with a primer and a probe, it is amplified by the qPCR machine. The amplification of the cDNA sequence is monitored throughout the steps of denaturation, annealing and extension, thus making this technique 'real-time'.

There are two main methods of cDNA detection: using intercalating dyes such SYBR Green, and probe-based methods (TaqMan). SYBR Green binds to any double stranded DNA present during each cycle of amplification. A TaqMan probe is an oligonucleotide strand that is conjugated with a fluorophore and a quencher. The fluorophore is released from the quencher during the PCR reaction through the exonuclease activity of the DNA polymerase. The released fluorophore can then be measured. We have applied this methodology for our MRD assays.

The specific cycle during qPCR at which a pre-set threshold is crossed is called threshold cycle (or Ct). The abundance of the target in the original cDNA determines the Ct value. The lower the Ct, the greater the amount of target present. To compare individual samples a housekeeping gene can be amplified in parallel and can then be used to normalize different samples with different amounts of starting material. One normalization method used is the ΔΔCt method. This method requires the PCR for the target gene and the PCR for the housekeeping gene to have very similar efficiencies. As this is usually not the case for PCRs used in MRD testing we must use a different method based on standard curves to normalize between individual samples. A detailed discussion of this methodology is included below.

While it is possible to detect molecular genetic aberrations in at least 80% of patients with AML, only a minority of them can be used for clinical routine testing as many of them have not yet been validated as MRD targets and as some of these genetic aberrations can also occur in clonal hematopoiesis (CH).

Humans have approximately 50,000 to 200,000 HSCs (Lee-Six H, 2018), wherein a single HSC can acquire 1 protein-coding mutation every 10 years, therefore, once an individual is 70 years old, up to 1.4 million protein-coding mutations can be acquired (Welch JS, 2012) (Jaiswal S, 2019). If one of the mutations can confer a greater fitness to the cell, according to the Darwinian selection, the cell can continue to expand. The cells arising from the initial mutated cell are called clones, if expansion of clones is present in HSCs, this is called clonal hematopoiesis (CH). The exonic mutations can closely resemble AML associated mutations, however, individuals with age-related CH do not always show signs of this blood cancer. Studies have found that DNMT3A, TET2, and ASXL1 mutations (DTA mutations) were common amongst age-related CH individuals (Raphael BJ, 2013) (Shlush LI, 2014). Studies have indicated that these DTA mutations are not good markers for relapse as they can persist after intensive treatment with no increase in risk of AML relapse. However, they can be eradicated following HCT (Wong HY, 2019) (Ivey A, 2016).

Sensitive routine assays that provide clinically relevant information have been developed for mutated NPM1 (mNPM1), which are discussed above and found present in 30% of AML samples as well as for the fusion genes found in CBF leukemia (CBFB-MYH11, RUNX-RUNX1T1) that are found in 5% and 7% of AML samples respectively. These clinical routine assays are RNA-based and have a very high sensitivity. They can detect 1 in 10^5 residual leukemia cells (Schuurhuis G, 2018). We have therefore established these assays in our lab to identify follow-up samples from leukemia patients containing MRD.

1.3.2 Multiparameter Flow cytometry and Fluorescence-Activated Cell Sorting

Flow cytometry is a technique used to identify different types of cells based on surface marker characteristics. Using a fluidics system cells are individualized and then pass by a laser. When the light scatters it results in forward scatter (FSC) and side scatter (SSC). FSC provides information regarding relative size of the cell which passes the light beam, while SSC specifies internal intricacy of each cell. Flow cytometry can also detect emitted light from excited fluorescent molecules, such as fluorescently labelled antibodies or other fluorescent stains. The antibodies attach to cell surface markers present on cells. Cell surface markers can identify lineage specific cells in hematopoiesis. These cell surface markers are termed according to the cluster of differentiation (CD) nomenclature. CD antigens can act as ligands, receptors, or cell adhesion molecules. For example, all leukocytes carry CD45 (Thomas, 1989).

In order to identify a specific cell population, multiple markers often have to be combined, which is possible in multiparameter flow-cytometry (MFCS). Using modern instrument, 8 or more individual markers can be detected simultaneously which then allows the detection of subpopulations of the analyzed cells. To identify individual markers, different fluorophores are utilized. When selecting appropriate fluorophores, the emission wavelength must be taken into consideration to avoid excessive spectral overlap. As well, dim fluorophores such as FITC, should be utilized for high abundance markers (CD34), while bright fluorophores such as PE should be used for low abundance markers (CD13) to increase discrimination of signal and background fluorescence. The fluorophore is excited by a laser and the emitted light is separated by wavelength using filters and mirrors and analyzed in photomultiplier tubes (PMT). The quantification of the relative amount of the fluorophore on a cell then facilitates its identification.

The detection of residual leukemia cells can then be facilitated by the identification of marker combinations that are usually not found in normal bone marrow. This is possible if the leukemia cells show an aberrant (cross-lineage) expression of markers, e. g. if they simultaneously express a myeloid marker profile with a lymphoid marker. As well, leukemia cells can be identified by the asynchronous expression of maturation markers. For example, if they either simultaneously express mature and immature markers or if they lack markers usually found together, such as CD13 and CD33 (Schuurhuis, et al., 2018).

Leukemia-associated immunophenotypes (LAIPs), and Different-from-Normal (DfN) are two approaches by which MRD cells can be identified. The LAIP method uses gates based on the initial leukemic population. The DfN method tries to detect the presence of aberrant phenotypes present in an individual sample by directly identifying cell populations not found in normal marrow. Some of the limitations of the LAIP-based detection of residual leukemic cells are the need for initial material to define the LAIP and the possibility for clonal evolution with a change in surface marker expression. The main disadvantage of the DfN method is a lower sensitivity. At present in clinical settings and for this project, a combination of the two approaches, a LAIP-based DfN method was recommended by the European LeukemiaNet (ELN) in 2018, and updated in 2021 to set the MRD detection cutoff value to 0.1% when using flow cytometry (Schuurhuis, et al., 2018).

This methodology has been successfully applied in the clinical setting (Freeman SD, 2018). The advantage of the MFC-based MRD assessment is that it can be applied to almost all patients with AML. The standardization of MRD panels has been attempted for numerous years. One of these approaches is the HARMONIZE consortium, which was established in 2016 to implement standards for MFC based MRD detection within two German AML study groups (SAL, AMLCG). The results of this effort have recently been published by Rohnert et al. The Harmonize consortium has developed an 8-colour MFC panel (shown in Table 2). A similar panel has been proposed by the ELN and with different fluorochrome-antibody combination is also used by other groups. The gating strategy used was based on fixed gates, only gates for doublet discrimination as well as recognition of lymphocytes were adjusted. In this strategy, a population including progenitors and monocytes is defined based on SSC and CD45. The population was identified to express at least one of the myeloid markers CD13 and CD33 and was then subdivided for the expression of CD34, CD117 and HLA-DR resulting in eight populations. These were then further characterized for the aberrancies: deficiency for CD13 or CD33 and aberrant expression of CD56 or CD7. The resulting strategy was tested on a cohort of 246 patients with AML. At follow up 64% of patients were identified as MRD positive based on the strategy described. The two-year OS was 92% for MRD negative patients and 63% for MRD positive patients. This difference was highly statistically significant, validating this strategy in a clinical setting (Rohnert M, 2020).

*Table 2. **.Harmonize multiparameter flow panel utilized for sort and flow experiments, presented with the fluorophores**. The MFC-MRD panel has been utilized in clinical settings, however, for this thesis this panel was used to isolate potential MRD cells. *Cross-lineage markers. **Asynchronous markers. † Early progenitor marker.*

Fluorophore	**FITC**	**PE**	**PErCP-Cy5.5**	**PE-Cy7**	**APC**	**AlexaFluor-750**	**Pacific Blue**	**V500**
Cell Surface marker	CD34†	CD13**	CD7*	CD33**†	CD56*	CD117†	HLADR**	CD45

1.4 Biology of Measurable Residual Disease

While huge advances have been made in the clinical use of MRD testing, our biological understanding of the processes that happen in MRD cells is unfortunately still relatively limited. Many biological investigations into MRD cells have so far been hampered by their low frequency. As they make up only about 1 in 10,000 to 1 in 100,000 of the cells in the bone marrow it is difficult to use any functional assays on these cells, as CFC, transplantation into immunodeficient mice, and even modern single-cell sequencing assays reach their limit of detection when the frequency of the population of interest is that low. However, as impressively demonstrated by the prognostic impact of MRD, these cells can give rise to relapse. It is therefore probably a relevant assumption that at least a subpopulation of MRD cells have properties of leukemic stem cells (LSCs). These LSCs have previously been characterized by their potential to give rise to leukemia when transferred into immunodeficient mice and have therefore also been called leukemia initiating cells (LICs) based on this potential (Thomas D, 2017) (Lapidot T, 1994). Original work in this field showed that LSCs are often found in a subgroup of leukemia cells that are characterized by specific immature markers (CD34+ CD38-) (Bonnet D, 1997), however more recent work suggests that LSC are even better defined by functional properties and a specific transcriptional profile (Ng S, 2016). Combining phenotypic stem cell markers with leukemia specific aberrant marker expression to identify residual AML cells with properties of LSC, has been suggested as one approach to enhance MRD detection (Schuurhuis G, 2018). However, as this would greatly reduce the number of detected cells, it can also lead to a reduction in the sensitivity of MRD testing. It is therefore important to understand what the functional properties of MRD cells are. The selective pressure during induction chemotherapy could select MRD cells for properties that make them resistant to chemotherapy, but these cells could also acquire resistance in a process called clonal evolution. Clonal evolution may follow distinct evolutionary models (Figure 2): linear evolution, and branching evolution. In linear evolution there is a sequential order of mutation acquisition. In branching evolution subclones with different properties can arise. Mutations present at diagnosis can be lost, and new mutations can be acquired. One of these subclones can then give rise to future relapse. The type of clonal evolution in an AML patient with disease progression can follow different patterns and depends greatly on the individual disease. Resistance mechanisms also do not depend on the acquisition of mutations but can also be the result of changes in transcriptional level. This has been found in the context of allogeneic stem cell transplantation (Christopher MJ, 2018). While LSCs were previously thought to be quiescent and chemotherapy resistant, recent studies have shown that LSCs are metabolically quite active and respond to treatment. Longitudinal studies performed on xenograft mice have also demonstrated that leukemic cells can transiently acquire properties that facilitate their regrowth. Regeneration of leukemia cells led to the formation of a transient cell population that was therefore called leukemia-regenerating cells, LRCs. This population of transient cells can contribute to relapse (Boyd, et al., 2018), but could also be targeted by treatment.

How common these described phenomena are in the treatment of patients is currently unknown and will require longitudinal studies in patients including studies on the MRD level. To facilitate these investigations, it will be necessary to comprehensively sort out MRD cells from patient's bone marrow and determine their characteristics by subjecting them to functional assays and in-depth characterization with single-cell sequencing approaches.

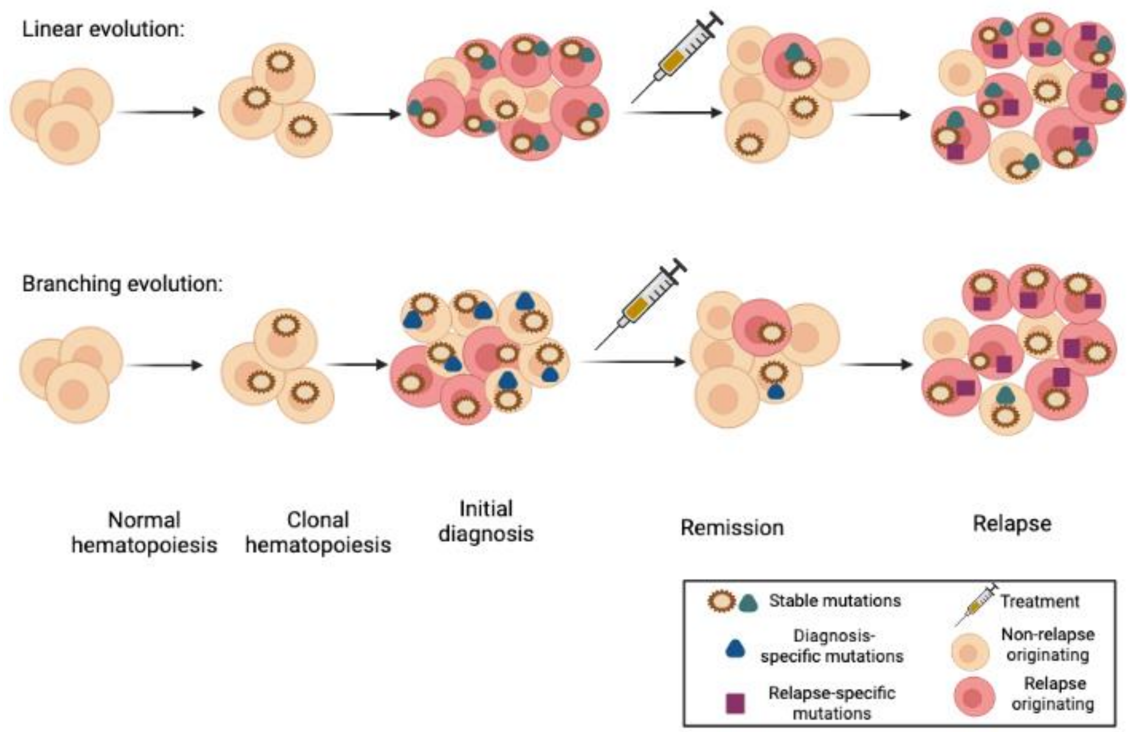

*Figure 2.**The two different methods of clonal evolution presented in AML.** The cells are presented in two colours, some do not have any mutations as they are wild type cells. The stable mutation in the cells remain consistent even after treatment, presented as a syringe. The yellow sun-like icon and green triangle represent stable mutations. The blue triangle represents a mutation only present at diagnosis, while the purple square represents a mutation gained after treatment. Linear evolution is described as a step process which involves gaining mutations. Branching mutations consists of a stable mutation similar to linear evolution, however, the initial diagnostic specific mutation is lost. The relapse clones arise from the initial diagnosis clones; considered subclones.*

1.5 Hypothesis and Aims

1.5.1 Rationale

MRD detection, as discussed above, has demonstrated its value in guiding clinicians in identifying patients at risk for relapse, which has found its way into the clinical decision making for patients with AML. However, investigations in the biology of MRD are essential to improve these approaches and to develop strategies to target MRD directly. MFC-based MRD detection could facilitate the prospective isolation of MRD cells, as it can be theoretically used for almost all AML patients without knowledge of molecular and cytogenetic abnormalities. However, the typical process used for clinical flow cytometry is incompatible with the use of the cells in downstream applications. In this thesis, we therefore aimed to modify a recently published MRD panel to develop a sorting strategy that can be applied to comprehensively enrich MRD cells from cryopreserved remission samples.

1.5.2 Hypothesis

We hypothesize that the clinical MFC strategy utilized for the identification of MRD cells can serve as a method to identify and sort MRD cells.

1.5.3 Specific Aims

1. Identify cryopreserved patient samples with detectable MRD using qPCR.
2. Identify a marker combination of interest that can be used in remission samples to enrich MRD cells by staining the diagnostic sample and compare different gating strategies
3. Apply the determined gating strategy to enrich viable MRD cells.
4. Determine and confirm the enrichment of MRD cells from aim 3 using qPCR.

Chapter 2: Materials and Methods

2.1.1 Patient samples

Our group is collecting longitudinal samples from patients with AML at different time points during treatment (Figure 3). The collection of these samples was approved by HIREB under project # 08-042-T. At diagnosis, either bone marrow (BM) or peripheral blood (PB) samples are collected, whereas for follow-up timepoints samples were collected from bone marrow. BM aspirates are more desirable, when investigating MRD, as compared to PB, as PB can be 5 to 10- fold less sensitive (Thol F., 2018). Samples were collected in tubes coated with ethylenediamine tetra-acetic acid (EDTA). The samples were then stored at 4°C until processing. Samples were processed within 72 hours of extraction to reduce cell attrition.

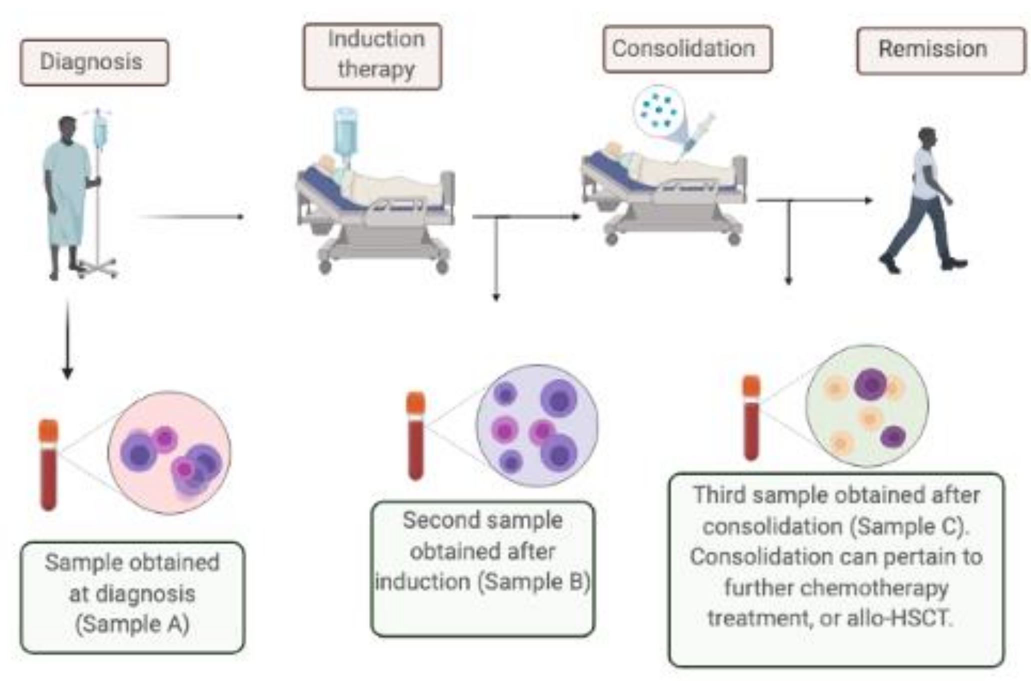

*Figure 3. **Longitudinal time points for AML patient sample collection.** The first blood sample obtained should be at diagnosis, followed by post-induction and post-consolidation. For this study only samples from patients with multiple longitudinal time points were used. Image developed on Biorender. AML: Acute myeloid leukemia, PB: Peripheral blood, BM: Bone marrow*

2.1.2 Sample Processing- Ficoll Density Gradient Centrifugation:

The dilution and washing buffer used for sample processing is abbreviated as P.E.F and composed of 97% PBS without salts, 1mM EDTA, and 3% FBS. The freezing media is composed of 90% FBS and 10 % dimethyl sulfoxide (DMSO).

First, the volume of blood was determined using a 5 mL serological pipette. The blood volume was then diluted with PEF at a final dilution factor of 1:4. After the dilution, we calculated the final volume (PEF + blood sample), and divided the final volume by 30 to obtain the number of 50 mL Falcon tubes needed for the Ficoll (Cytiva) density gradient. Once the number of 50 mL tubes was determined, 15 mL (or 50 % of the volume of the diluted sample) Ficoll was added to the bottom of the 50 mL tube, and the indicated diluted sample was very slowly layered on top of the Ficoll. The tube was tilted on its side, and the diluted blood sample was added with a 50 mL serological pipet. These steps were taken to ensure no disruption occurred to the Ficoll barrier. The sample was then centrifuged for 20 minutes at 1500 RPM with break and acceleration set to minimum. After this centrifugation, four visible layers were seen: the red blood cells presented at the bottom as a pellet, the Ficoll as the second layer, the mononuclear layer, followed by the plasma. The mononuclear cell layer was slowly harvested using a 2 mL serological pipette and transferred into a fresh sterile 50 mL tube. The removed mononuclear cells were then centrifuged at 1500 RPM for 5 minutes, with break and acceleration set back to maximum. After centrifugation, the supernatant was removed and the pellet was resuspended in 10 mL of ammonium chloride (StemCell Technologies) and incubated for 10 minutes at room temperature to lyse the red blood cells remaining in the sample. Following this incubation period, 20 mL of PEF was added to neutralize the ammonium chloride. This was again followed by a centrifugation step at 1500 RPM for 5 minutes. The supernatant was removed, and the sample was resuspended in an appropriate volume of PEF for the cell count. Once the resuspension was completed, the cells were counted by adding 20 µL of the sample into an Eppendorf tube and combined with 20 µL of Trypan blue (Thermo Fisher). 10 µL of the mixture was pipetted into a counting chamber and inserted into the Countess 3 Automated Cell Counter (Thermo Fisher). The total cell number was calculated for cryopreservation. We aimed to cryopreserve in aliquots of $5x10^6$ cells and, if possible, $20x10^6$ cells per vial. After counting, the cells were spun down at 1500 RPM for 5 minutes and resuspended in freezing media. The samples were then placed in a freezing container overnight at -80 ºC, and then transferred to a -150 ºC freezer with liquid nitrogen backup.

2.3 RNA isolation and qPCR

RNA extraction was performed using the Qiagen RNeasy Mini or Micro Kit (Qiagen, Toronto, Canada) depending on the number of cells used.

2.3.1 RNA Isolation with Qiagen RNeasy Mini Kit

Cells were lysed in 350 µL of activated buffer RLT. To activate buffer RLT, 10 µL of B-mercaptoethanol (Thermo Fisher) were added to every 1 mL of Buffer RLT. After pelleting the cells, 350 µL of activated buffer RLT were added and vortexed for 30 seconds. 1 volume of 70 % ethanol (350 µL) was added to the lysate and mixed by pipetting. The 700 µL volume was transferred to a RNeasy spin column. The column was centrifuged for 15 seconds at 11,000 RPM in an Eppendorf Mini centrifuge. The flow-through was discarded. The column was then washed with 700 µL of buffer RW1 and centrifuged for 15 seconds again at 11,000 RPM. The column was then washed twice by adding 500 µL of Buffer RPE to the spin column and spun down at 11,000 RPM for 15 seconds and 2 min respectively. After discarding the flow-through, the column was spun once more to dry the membrane (14,000 RPM for 1 minute). To elute the RNA, 30 µL of nuclease free water (NFW) was added directly to the column and allowed to incubate for 2 minutes before spinning down for 1 minute at 11,000 RPM to collect the eluted RNA. This elution was repeated once more using the same NFW already containing the previously eluted RNA. RNA concentration and purity were analyzed using a Nanodrop spectrophotometer (Thermo Fisher).

2.3.2 RNA Isolation with Qiagen RNeasy Micro kit

This preparation method was used for cell populations of less than 1x 10^4 cells. DNase I (Qiagen) stock was dissolved in 550 µL of NFW. The volume of NFW was injected with 100 U insulin syringe, and the vial was inverted to mix. The stock was divided into single-use aliquots of 20 µL and stored in -20 ºC. The pelleted cells were lysed using 350 µL of activated Buffer RLT as per 2.3.1. After homogenizing the pellet, 350 µL of 70% ethanol was added and mixed by pipetting. The entire volume (700 µL) was added to an RNeasy MinElute column, and spun at 10,000 RPM for 15 seconds. The flow-through was discarded. 350 µL of Buffer RW1 were added, and the column was again centrifuged at 10,000 RPM for 15 seconds, the flow-through was discarded once more. We then combined 10 µL of DNase I stock, and 70 µL of Buffer RDD, added the whole 80 µL to each column. The column was allowed to sit at room temperature for 15 minutes. Once the incubation period was over, 350 µL of Buffer RW1 were added, and the columns were spun down at 10,000 RPM for 15 seconds. The collection tube was replaced by a fresh 2 mL tube. 500 µL of Buffer RPE was added to the column and spun down at 10,000 RPM for 15 seconds. The flow-through was discarded. This was followed by the addition of 500 µL of 80% ethanol, and the RNeasy MinElute column was spun down at 11,000 RPM for 2 minutes. The flow-through was discarded. To ensure that the membrane was dry, the column was spun down at maximum speed (14,000 RPM) for 5 minutes. The column was then placed in a 1.5 mL Eppendorf tube for elution. 14 µL of NFW was directly added to the centre of the spin column. This was allowed to rest for 1 min before spinning down at 14,000 RPM for 1 min. The elution was completed once more using the already eluted volume for maximum efficiency. The RNA concentration and purity were again determined using a Nanodrop spectrophotometer.

2.3.3 cDNA synthesis

The cDNA synthesis utilized a maximum of 1 µg of the sample RNA (in a maximum of 5.1 µL volume). Superscript Vilo Master Mix (Vilo MM, Thermo Fisher) was utilized due to its high reverse transcriptase (RT) efficiency. Before Vilo MM was added, the sample was heated to 70 ºC in a heat block for 10 minutes and placed on ice for 5 minutes. A single reaction for cDNA synthesis required 4 µL of Vilo MM, added to 5.1 µL of RNA, and topped to 20 µL with nuclease free water (NFW). The mixture was placed in a thermocycler, incubating at 25ºC for 10 minutes, followed by 42ºC for 60 minutes, and finally 85ºC for 5 minutes. The obtained cDNA was then stored at -20ºC.

2.3.4 Quantitative PCR

Quantitative PCR was performed using the Ipsogen NPM1 mutation A MutaQuant kit (Qiagen) for patients with Type A, or using Qiagen Ipsogen NPM1 mutations B&D MutaQuant kit (Qiagen) for patients with an NPM1 type B and D. The Ipsogen RUNX1-RUNX1T1 kit was used for patients with RUNX1-RUNX1T1. Patient 13156 had a rare NPM1 mutation in which a 4-base pair insertion (TTTG) was detected at position 863_864 on chromosome 5 exon 12. For this patient, a new standard was designed to allow quantification of *NPM1-TTTG (*described below).

To facilitate quantification, samples were normalized using ABL as housekeeping gene. 12.5 µL of Taqman Fast Advanced master mix (ThermoFisher), 6.5 µL of NFW, and 1 µL of the primer/probe were combined (provided with Ipsogen kit). This master mix was then combined with 5 µL of the sample to a total volume of 25 µL. After pipetting the samples and the master mix into each well, the 96 well plate was covered with a plate seal. The plate was centrifuged for 30 seconds at 1000 RPM. Each reaction was run in three replicates. For the Ipsogen kits, TAMRA was selected as the quencher and FAM as the reporter dye. For the NPM1-TTTG, the qPCR quencher was NFQ-MGB. The program for the NPM1 kit provided by Qiagen was 50 ºC for 2 mins, followed by 90 ºC for 10 mins, then 50 x cycle of 95 ºC for 15 seconds, and 63 ºC for 1 minute (for the NPM1-TTTG this was 60 ºC for 1 minute). The resulting cycle-threshold values (Ct) for each technical replicate (n=3) of a sample were averaged. To facilitate normalization of samples, the standard curve method was used. The Ipsogen kits contained standards with serially diluted defined copy numbers for the respective target mutation and for the housekeeping gene. The Ct values were standardized by first calculating the regression line for both the ABL and NPM1 standards. The derived line equations could then be used to calculate the copy numbers for the target gene (NPM1 mutation, RUNX1-RUNX1T1) and ABL for each of the samples. Once this was done, the equations of the lines were used to find the log of the copy number for each of the samples, and then the copy number. Finally, the copy number of the NPM1 was divided by the copy number of its ABL control (Figure 4). As the ratio of mutant NPM1/ABL can be assumed to be equal in all cells of the leukemic sample, this ratio can then be used to draw conclusions about the content of leukemic cells in the analyzed sample.

A

Sample Name (NPM1)	Average Cycle-Threshold Value	log(CN)	CN
Sample A	33.74	1.94	87.94

B

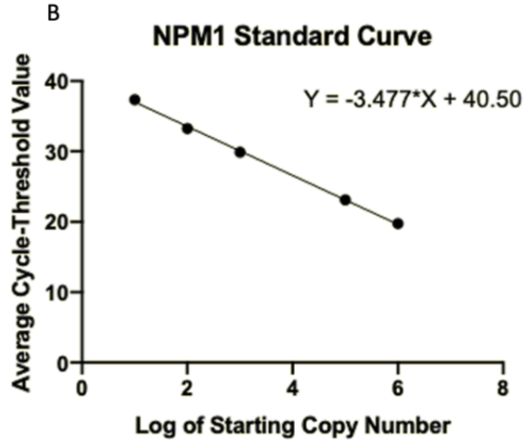

C

$Y= - 3.477*X+ 40.50$
$(33.74-40.50)/-3.477= X$
$X= Log(Copy\ Number)$
$X= 1.94$

10^x = Copy number
$10^{1.94} = 87.94$

*Figure 4. **The qPCR standardization and copy number identification steps.** First, the average cycle-threshold was calculated (A), followed by identifying the equation for the line of regression (B), and then calculating the log of the copy number. Finally, the copy number was calculated (C).*

2.4 Cloning and dilution of the NPM1-TTTG Standard

Patient 13156 has a rare NPM1 mutation wherein an insertion within exon 12 has occurred (863_864insTTTG). As we had multiple longitudinal samples from this patient at various time points after treatment, a qPCR assay for this mutation has been adapted from the literature (Mencia-Trinchant N., 2017). To facilitate its use in analogy to the commercially available assays, a standard had to be established by cloning the PCR product of this patient sample and diluting it to defined concentrations.

We first thawed one vial of primary cells in 85% Iscove's modified Dulbecco's medium (IMDM), supplemented with 15% fetal bovine serum (FBS), spun down at 1500 RPM for 5 minutes. The sample was then resuspended in Dulbecco's Phosphate Buffered Saline (DPBS, Fisher Scientific), and counted using a Countess 3 Automated Cell Counter (Thermo Fischer). The sample was then subjected to RNA extraction and cDNA synthesis as described above. A gradient PCR with 5 annealing temperatures was then performed to identify the optimal annealing temperature. The product was then analyzed by agarose gel electrophoresis on a 2 % agarose gel in Tris-Acetate-EDTA (TAE) buffer. Nucleic acids were visualized using RedSafe Nucleic Acid (FroggaBio) staining solution. In addition to the PCR products 5 µL of DNA 1kb ladder (ThermoFisher) run to confirm the right product size and optimal PCR condition. The optimal annealing temperature was 53.5 ºC. Following the PCR gradient, another PCR was performed with the annealing temperature set at 53.5 ºC, all else remaining the same (See Appendix B).

The product of this PCR was then transformed using the TOPO Blunt II kit (Figure 5). For the transformation, 4 reactions were set up with different amounts of PCR product to ensure that a single, non-clustered, colony was obtained.

Reaction 1 contained 1 µL of PCR product, reaction 2 contained 2 µL of PCR product, and reaction 3 and 4 consisted of 4 µL of PCR product. 1 µL of TOPO Blunt II, 1 µL of salt solution supplied, PCR product according to previously stated reaction, and up to 6 µL of water were combined for each reaction. The reactions were incubated at room temperature for 5 minutes, then placed on ice. Transformation was performed using freshly thawed vials of OneShot Stbl3 competent cells and DH5α competent cells. 2 µL of the cloning reactions were added to each of the 3 OneShot Stbl3 competent cells, and 2 µL of the reaction 4 was added to 50 µL of DH5α competent cells. The mixture was placed on the ice for 7 minutes (5-30 minutes). The reactions were placed in heating block at 42 °C for 30 seconds. Immediately following the heat-shock, 250 µL of room temperature SOC media was added to the mixtures. The transformed cells were placed on a shaker for 1 hour at 37°C. Finally, 50 µL of the reactions were then spread on prewarmed Luria-Bertani (LB) plates with 50 ug/ml of kanamycin, placed overnight at 37°C. The next morning, 9 colonies were selected for plasmid isolation. The plasmids for each of the colonies were isolated with the Qiaprep Miniprep Kit (Qiagen). To confirm the correct insert, the colonies were sequenced with M13 forward and reverse primers (See Appendix B Table 3). The results showed that three of the nine samples sent had the correct sequence and orientation. Two of these three colonies were used to develop the standards. The development of the standard followed the protocol suggested by ThermoFisher Plasmid Standard (ThermoFisher, 2003). The plasmid was first diluted to 2.0 µg/µL in order to follow the protocol efficiently. Both colonies underwent the following calculations. The goal was to develop a standard containing different concentrations of the target sequence from 1 million copies to 10 copies (1 million, 100,000, 10,000, 1,000, 100, 10). The mass of a single plasmid molecule can be estimated using the following equation:

$$m = plasmid\ size\ (bp) \times 1.096e - 21$$

As the total plasmid size was 3600 bp (3500 bp plasmid + 100 bp insert). The mass of a single molecule was 0.394e-21 grams. Following this calculation, we then calculated the mass of plasmids containing the copy numbers of interest. As a sample calculation, below is the calculation of 1 million copies.

$$0.394e - 21\ \times\ (1 \times 10^{6}) = 0.394e - 11\ grams$$

The mass of the plasmid DNA required was then calculated for all the copy numbers. The mass of the plasmid DNA was then divided by the volume to be pipetted (5 µL). The final concentration was then established. Finally, the serial dilutions were prepared using the final concentration of the 1 million copy number, as shown below.

$$(2 \times 10^{-12}) \times\ V = (7.88 \times 10^{-13}) \times\ 100\ uL$$

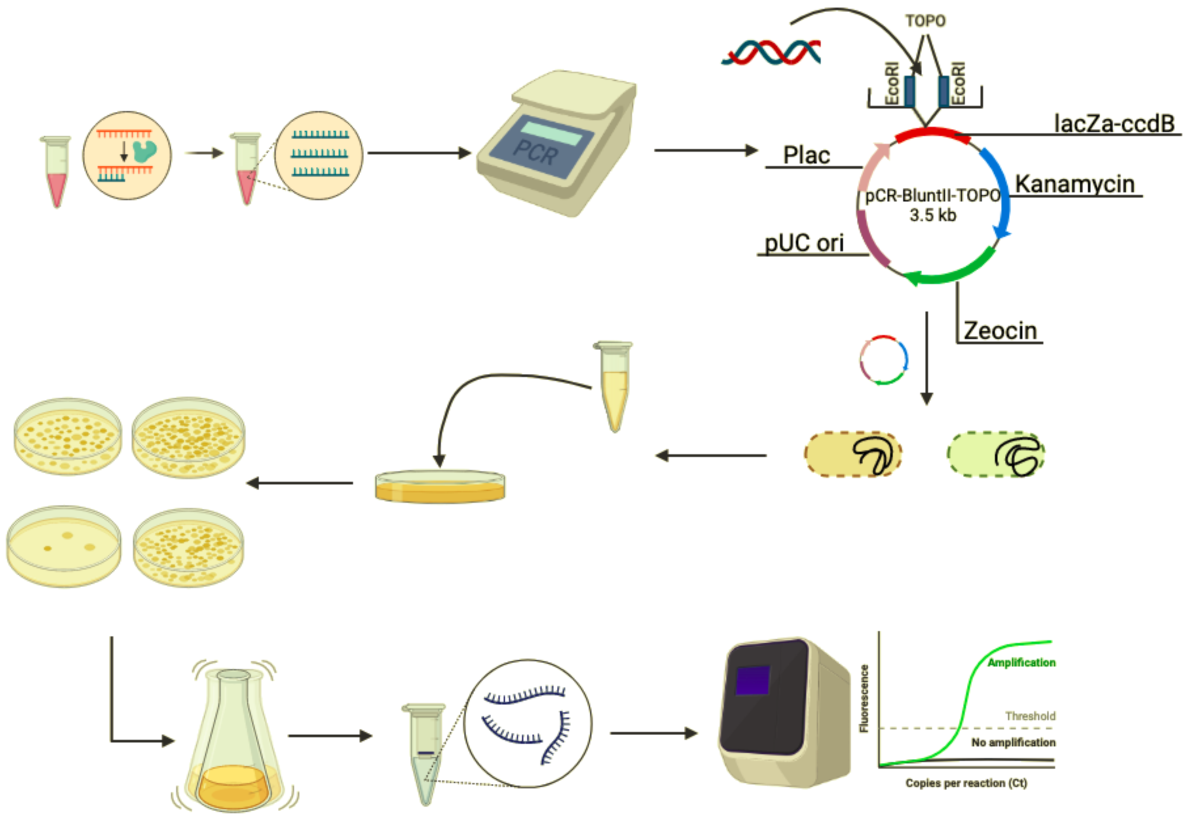

Figure 5. ***Workflow for development of new standards for NPM1-TTTG mutation****. Topo Blunt II was utilized for transformation. Stbl3 competent cell is indicated as the yellow cell, while the DH5α competent cell is indicated in green. After performing heat shock, the cells were transferred growth media in different concentrations. The colonies grew overnight and a few were selected for expansion in overnight culture. The next morning, the selected colonies underwent plasmid isolation. After confirmation by sequencing, the standard was then used for qPCR.*

2.5 Preparation of samples for flow cytometry

MRD wash buffer (PBS + 0.2% BSA, filter sterilized) was prepared in advance.

The preparation of samples for flow cytometry (MFC) and sorting (FACS) followed similar steps. A vial of 5 million cells/ mL (20 million cells/ mL where appropriate for sorting) was thawed and pipetted drop by drop to 10 mL of PEF. This was centrifuged at 1500 RPM for 5 minutes. Meanwhile Falcon polystyrene flow cytometry tubes were prepared. Since MFC and FACS were performed on two different samples (ie. Diagnosis, Post-chemotherapy), the patient sample was indicated on the label as A for diagnosis and B/C/D as a follow up sample, depending on the time point of sample extraction. Therefore, for a patient with an A and B sample, there were four total tubes; unstained, live dead stain, stained sample A, and stained sample B.

The supernatant was removed, and the cells were resuspended in 2 mL of PEF for counting via Trypan blue exclusion. The cells were then filtered using the Falcon round-bottom polystyrene test tubes with 0.35 µm cell strainer cap. 20 µL of the sample, and 20 µL of Trypan Blue were combined in an Eppendorf tube, and 10 µL was pipetted into a slide to be counted by the cell Countess 3 automated cell counter. After counting, 100,000 (50,000 cells for MFC) cells from the diagnosis sample were removed from the stock for the unstained, live dead stain tubes. 50,000 cells were removed for each of the fluorescence minus one (FMO) controls for FACS. The remaining cells were used for the sample FACS (200,000 cells were set aside for qPCR if performing MFC). Following the separation of the cells in their appropriate tubes, the cells were diluted by PEF up to 2 mL and centrifuged at 1500 RPM for 5 mins. Meanwhile, the BD CompBeads were prepared. Two drops of the beads were pipetted into each round-bottom polystyrene tube. A single antibody was added into each tube, therefore, a total of 9 compensation controls were generated. For staining 5 µL of each antibody was used.

The supernatant of the sample tubes was removed very carefully. The sample tubes were each suspended in 100 µL of PEF (for FACS, unstained and live dead stain were suspended in 400 uL of PEF), and 5 µL of every antibody was added, except for unstained and Live-Dead Red. 4 µL of 7AAD (live dead stain) was used for every 200 µL (1/50 dilution), and this was added at the end of preparation. 7AAD did not require additional washing steps, as such it was added immediately before experiments. The CD7 antibody could be omitted for the sorting as the 3 samples analyzed did not show aberrant CD7 expression in a high fraction of cells. The beads and the samples were incubated for 20 minutes at room temperature protected from light, 7AAD was not incubated and added as close as possible to the time of MFC and FACS analysis. Collection tubes for sorting were prepared by coating the wall of opaque round-bottom sorting tubes with 100% FBS and adding 800 µL of PEF into each.

After the incubation, 2 mL of MRD wash buffer was added the cells and beads with antibodies and centrifuged at 1500 RPM for 5 minutes. After removal of the supernatants, the beads were set aside and the cells were washed once more with 2 mL of MRD wash buffer. After this final centrifugation step, the supernatant was removed, and the pellet was resuspended in 200 µL of PEF. The samples were then analyzed on a Beckman Coulter CytoFlex LX instrument.

2.6 Gating for Flow Cytometry and Determination of Enrichment Strategy

The obtained FCS files were analyzed in the software FlowJo™ v10.8 to identify patient specific MRD phenotypes. A hierarchical gating strategy has been utilized in our work to enrich for MRD cells, the gates summarized in Figure 6 were used to determine the phenotype that would include most of the original leukemic population. The hierarchical gating strategy used in MFC initiated with doublet discrimination (selection of single cells) based on SSC-Area and SSC-Width/Height. Cells remain in a linear path on the graph (diagonal), while doublets will tend to present double the area. The single cells were then gated for live cells with the aid of a fluorophore dye penetrating dead cells (7AAD, Live-Dead Red). Since dead cells are stained by the dye, the gate will encompass cells that present minimal fluorescence, as these are the live cells. A similar gating strategy was also applied for sorting based on the availability of cells 5,000-100,000 live cells were collected; for the samples with limited number of cells only 5,000 cells were obtained. The limit for these initial cell collections were placed in order to ensure that enough cells remained for the collection of the population of interest. The next gate to be placed on single, live cells was the selection of blasts with the use of side scatter and the cell surface marker CD45 (V500). CD45 is present on the majority of hematopoietic cells and the level of CD45 in combination with the side scatter can aid in separating blasts from other populations, although contamination of other cells in the blast population is still possible (Harrington A, 2012). Erythrocytes present low amounts or altogether missing expression of CD45, while monocytes (high SSC) and lymphocytes present greater expression of CD45, and granulocytes present CD45-dim, and high SSC. The blast gate was placed at a region between erythrocytes, and monocytes and lymphocytes, in which CD45-dim, low SSC is present. For some leukemic samples this gate was expanded to include a monocytic population. Following gating for blasts, the cells were then gated either for a myeloid progenitor marker combination or an aberrant phenotype identified on the blast. The gates were based on the diagnosis sample and applied to the follow up sample. We collected 5000-10,000 live blasts for the FACS experiments, concurrently collecting remaining cells that did not fall in the blast gate; termed NOT blasts.

The phenotype of the leukemic cells was then determined based on the simultaneous assessment of the expression of CD33 (for myeloid cell identification) and the other markers (CD117, CD34, CD13, CD7, CD56 and HLA-DR) studied. Whereas the combination of CD117 and CD34 with CD33 allows the identification of myeloid progenitor cells, the combination of CD7 and CD56 would allow for the identification of aberrant expression of these two lymphoid markers. The simultaneous examination of CD33 with HLA-DR and CD13 allows for the identification of asynchronous expression of these maturation markers; based on absence of these cell surface markers (HLA-DR, CD13). "True" LAIP strategies usually require the Boolean combination of these gates and exclusion using different normal samples to determine a phenotype, that is usually only found with a maximum frequency of 0.1% (Schuurhuis G, 2018). This strategy proved too stringent for an enrichment sorting strategy, as it would often only include a minority of leukemic cells and as the enrichment for our purposes should provide a sufficient number of cells to be used for qPCR, and future molecular assays. We therefore only determined for the individual combination of CD33 with the respective marker if an aberrant or immature phenotype was found in the original leukemia sample. To identify whether the gates placed on the samples was appropriate, lymphocytes were used as an internal control. The gates were dictated by comparing the patient sample's own lymphocytes with myeloid blasts (Figure 6). The gates were fixed, and the only gates changed were doublet discrimination, debris exclusion, and blast selection. Four categories of aberrant populations were identified: deficiency of CD13 or CD33 and cross-lineage expression of CD56 or CD7. Myeloid progenitor populations (MPMs) were also investigated as possible phenotypes. The same gates for the samples were placed on the controls to obtain percentage of the population within the gates. The aberrant/immature gate used for sorting was chosen based on the combination that represented the highest fraction of phenotype cells in the original leukemia sample relative to the total of live CD45+ cells in the sample.

2.6.1 Sorting of Populations of Interests

After determining the populations of interest, cell sorting was performed on a BD FACSARIA II cell sorter. For the final sort, 4-way sorting was used to obtain the cells with the phenotype of interest as well as control populations either not falling into the blast gate (NOT blast), and cells that did not fall into the phenotype of interest (NOT Phenotype). As such, for each patient sample sort, 3 total sorts were performed to obtain the following populations: total population (live only), NOT blast, blast, Phenotype, and NOT Phenotype.

Figure 6. ***The gating strategy utilized for LAIP/MPM- based MRD detection.*** *Blast (blue) and lymphocytes (orange) were identified in patients using SSC/CD45. Myeloid progenitor markers(MPMs)are identified in the top two panels. The bottom three panels demonstrate the aberrant populations distinguished by four categories. Patient lymphocytes were considered as controls.*

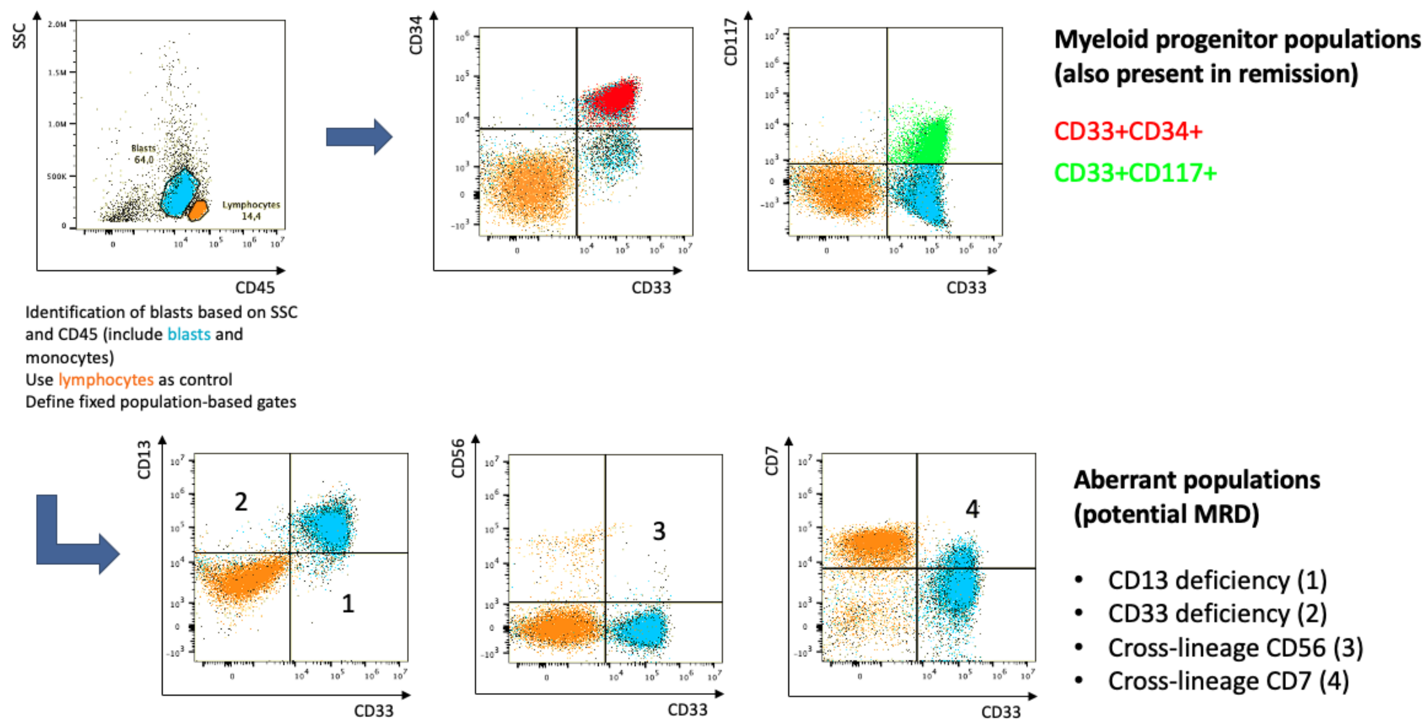

2.6.2 Determination of Enrichment

To determine if the sorting led to an enrichment of leukemic cells qPCR for the mutation found in the leukemia was performed on the sorted populations. The sorted cell populations were subjected to RNA isolation using the protocols described above for limited numbers of cells (RNeasy Micro Kit, Qiagen). The obtained RNA was then subjected to qPCR for the target gene of interest. ABL1 was used as a housekeeping gene. We again calculated copy numbers of the target gene-of-interest. These were then normalized using the transcript copy number of ABL1. As described above for the determination of MRD, this NPM1/ABL ratio (normalized NPM1 copies) correlates with the frequency of MRD cells in the sorted populations and therefore allows to determine if this frequency is increased by the respective sorting. The ratio between the normalized NPM1 copies in the sorted population (Phenotype) and the unsorted population (Live only) was used to determine by which factor the MRD could be enriched through the sorting. The comparison to the NOT Phenotype cells were used to determine how much of the leukemia cells were left behind in the flow-through.

Chapter 3: Results

3.1 Identifying Patient Samples with Potential MRD

3.1.1 Sample processing of longitudinal samples from patients with AML

Samples from 86 patients with AML were collected and processed for the HHS McMaster Stem Cell Bank. Patient samples were selected based on criteria that make them suitable for these experiments (Figure 7).

Initially, the patient samples were evaluated based on the availability of follow-up samples. For our work, longitudinal samples from patients were necessary to evaluate the presence of MRD as they are compared to diagnosis samples. From the 86 AML patients, 36 had longitudinal samples submitted to the cell bank.

The second criterion was established to identify patients with molecular suitable for MRD detection (ex. NPM1, RUNX1-RUNX1T1). For 8 patients we had longitudinal samples in the cell bank that possessed suitable molecular MRD markers. The information about molecular markers were based on clinical annotation information in the cell bank database.

We also had to consider, which samples had adequate number of cells available for the planned analyses. To determine the presence of MRD by qPCR and perform preliminary MFC analyses approximately 5-10 x 10^6 cells per experiment were needed. Follow up sorting experiments required additional cells (up to 20 x 10^6 cells per experiment depending on sample viability).

Based on these criteria, we identified samples from 7 patients and analyzed them for detectable MRD.

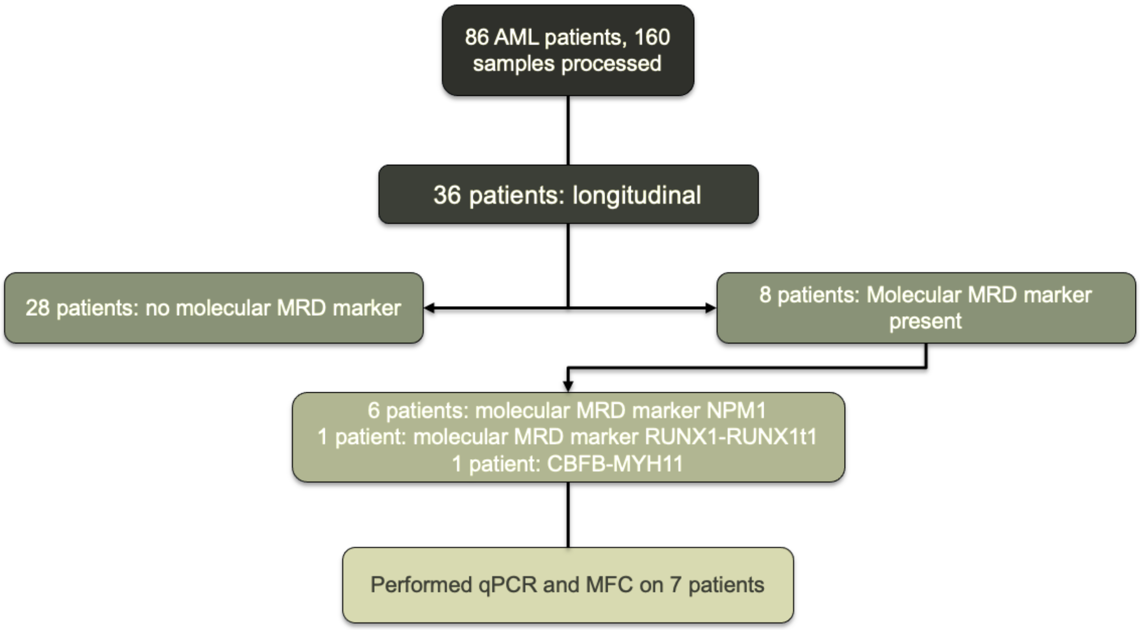

Figure 7. ***Processed patient sample breakdown, and selection of patients with potential MRD****. Molecular MRD marker represents stable markers for which sensitive assays are available. The patient samples with molecular MRD markers were processed for qPCR to identify presence of MRD in follow-up samples.*

3.1.2 Identification of MRD Positive Follow-Up Samples

As the selected patient samples had molecular markers that allow for MRD detection, qPCR could be used to identify samples with detectable MRD. The criterion for detectable MRD followed recent recommendations by the ELN for MRD detection. Samples were considered positive for MRD if there was a level of > 200 copies of the respective molecular marker / 10^4 ABL copies. Samples exhibiting < 100 - 200 copies / 10^4 ABL copies based on these criteria are classified as molecular persistence at low copy number, or complete remission.
To establish the qPCR assay and to determine its sensitivity defined dilutions of cells from cell lines were used (See Appendix A). We used the cell line OCI-AML3 for this purpose. This cell line carries a type A NPM1 mutation. Cells from this cell line were mixed with cells from the cell line HL60, that are negative for this mutation. Based on criteria outlined above a sample with 200 copies of the target /10^4 ABL copies contains 0.14 % NPM1-mutated cells (or approximately 1.4 NPM1-mutated cells per 1,000 cells).

This sensitive qPCR assay and analogous assays for other types of NPM1 mutations and RUNX1-RUNX1T1 were used to determine the MRD status of samples from 7 patients based on the criteria discussed previously. The result of the qPCR is demonstrated by transcript copy number of the target gene and ABL endogenous control as well as the ratio of copy number of the target / 10^4 copies of ABL (Table 3). As mentioned previously, the results are sectioned based on the level of MRD detected. Patient samples with > 200 target copy number/10^4 ABL copies were considered to be MRD positive. The patient molecular mutations and cytogenetics presented were derived from the annotation information in the cell bank. The diagnosis sample source is indicated; all the follow-up samples were from BM aspirates. For some patients from the list, only follow up samples were available. Follow up samples from three patients were considered as MRD positive. These are the samples from patients 13156, 22005, and 21029. Even though reagents used also for clinical testing were used for these experiments, the results obtained would not fulfill the standards expected for clinical MRD testing. In this setting, an accredited process would be expected. We also saw a high variability in the copy number of ABL detected. This most likely has to be attributed to a low sample viability in some of the samples, potentially because of storage time and/ or delays in RNA isolation. Based on recent ELN recommendations, a copy number for ABL > 10^4 is usually expected in clinical testing (Heuser M., 2021). This criterion was fulfilled for some, but not all samples analyzed. At the time when the assay for patient 13156 was performed, we also did not have the standard available for quantification, the result of the PCR reported here would therefore have to be considered qualitative. This standard was then developed and used for subsequent analysis using sorted cells (see below and in the methods section). Based on the Ct value, the PCR for the follow up sample was estimated to be positive, which was also confirmed when analyzing sorted live cells from this patient (1888 copies target gene/ 10^4 copies ABL). The obtained results were therefore still sufficient to determine that three patients (13156, 21029, and 22005) had MRD positive follow up samples. Diagnosis samples and follow up samples from these patients were therefore evaluated by MFC to identify the most suitable cell surface marker combination for sorting MRD cells from these samples.

Table 3. Summary of patient MRD status obtained using RT-PCR using ABL gene as the endogenous control. The target gene is indicated and quantified along with the ABL control gene. Complete remission was defined as obtaining undetermined target gene copies, or status was obtained from a third party. Molecular persistence at low copy number was defined as <100-200 copies /10^4 ABL copies. If the qPCR resulted in an undetermined value, the sample was placed under insufficient information .All samples were run in triplicates, including water control.

**No diagnosis obtained.*

***Two diagnosis samples were obtained; indicated as A and B. B was used for this study as it was leukapheresis.*

†Disease status was based on annotation information from the cell bank.

Sample ID	MRD target	Sample Treatment Status	Quantification of target gene (represented as copy number)	Quantification of ABL endogenous control (represented as copy number)	Copies of target gene/10^4 copies ABL	Source	Cytogenetics	Molecular Mutations
Complete Remission (Negative)								
21054	NPM1 (Type B)	A: Diagnosis B: Post-Induction	A: 1126.38 B: 0 (CT>40)	A: 18555.27 B: 15249.16	A:607.04 B: 0	PB	46, XY[20]	NPM1 (c.863_864insCATG)
18469	RUNX1-RUNX1T1	A; Diagnosis B: Post-Induction C: Post-Consolidation I D: Post-Consolidation II	A: 16.12 B/C/D: 0 (CT>40)	A: 3.33 B: 626.10 C: 129.81 D: 4068.04	A:48408.4 B/C/D:0	BM	45, XX, t (8;21) (q22; q22) [18]/46,XX[2]	RUNX1-RUNX1T1
Molecular persistence at low copy number								
21027	NPM1 (Type D)	A: Follow-up B: Follow-up	A: 79.49 B: 10.12	A: 16544.45 B: 5954.94	A:48.05 B:16.99	BM	46, XY [20]	NPM1 (c.863_864insTCTG), FLT3-ITD
22004*	NPM1 (Type B)	B: Induction I C: post-consolidation I D: post-Consolidation II	B: 19.78 C: 16.40	B:22557.34 C: 12923.17	B:8.768 C:12.69	BM	46, XX[16]	NPM1 (c.863_864insCATG)
Molecular Persistence/ MRD positive								
21029**	NPM1 (Type A)	B: Diagnosis D: post-induction II E: post-consolidation F: post-consolidation II	B:12775.21 D:249.93 E: 111.75 F: 16.5	B: 3599.48 D: 307.04 E: 2515.77 F: 162.23	B:35,491.2 D:8139.98 E: 444.19 F:1,015.07	PB	46, XY[20]	NPM1 (c.863_864insTCTG), FLT3-ITD
22005	NPM1 (Type B)	A: Diagnosis B: Post-Induction	A: 1041.53 B: 11096.9	A: 21467.42 B: 18286.15	A: 485.17 B:6068.47	PB	46, XX [5] and then 46,XX[15]	NPM1 (c.863_864insCATG)
Undetermined (qualitative positive)								
13156	NPM1-TTTG	A: Diagnosis B: post-induction C: post-consolidation	CT value A: 25.45 CT Value C: 30.03	CT value A: 28.74 CT value C:30.77	NA	PB	46, XY	NPM1(c.863_864insTTTG), FLT3-TKD

3.3 Determination of the Phenotypes Suitable for MRD Enrichment

As described above, diagnosis and follow up samples identified to be positive for MRD by qPCR were analyzed by MFC. This immunophenotypic analysis used a clinical MRD panel originally proposed and recently published by the HARMONIZE consortium (Rohnert M, 2020). The specific task to enrich for MRD cells would require modification to the protocol to use samples that have undergone mononuclear cell isolation and cryopreservation. As these cryopreserved samples can have a variable viability it was also relevant to include a viability dye in the staining. The gating strategy chosen for this purpose would also need to be different from a clinical MRD strategy to assure inclusion of a maximal fraction of the original leukemic population. Similar to the gating strategy used by the HARMONIZE consortium a fixed gating strategy was used. The gate for single cells, viable cells and blasts was determined based on the diagnostic sample and were then applied to the follow up samples. The HARMONIZE consortium uses a gating strategy to identify flow cytometric MRD that combines the presence of immature markers (CD34, CD117. HLA-DR) with one of 4 aberrations identifiable using the panel (aberrant expression of CD7, aberrant expression of CD 56, deficiency of CD13 or deficiency of CD33). This then results in a total of 32 possible abnormal populations. While these can potentially be very leukemia-specific based on a very low fraction of a marker combination found in a normal bone marrow, each of these marker combinations would only make up a relatively low fraction of the leukemic cells at diagnosis. Our challenge was therefore to identify gates that are specific enough to enrich for leukemic cells but would also include the highest possible fraction of residual leukemic cells in a given sample.

To arrive at the most appropriate sorting strategy for an individual leukemia patient, we therefore now determined which aberrant or immature cell population was most frequent in the diagnostic sample (Table 4).

For patient 13156, $CD33^{+}CD34^{+}$ cells made up the greatest percentage at diagnosis, 61.01%. The percentages were calculated by dividing the cell population by the live cell population. Other immature or aberrant cell populations made up only small fraction of leukemic cells.

Patient 21029 presented only a lower fraction of CD34 positive cells, but a high percentage of $CD33^+CD117^+$ cells was found (42.01 %). The original population also had a relatively high level of CD33+CD7+ cells (46.77%), however there was a reduction of this population after the first induction cycle while the CD33+CD117+ population was maintained. This myeloid progenitor marker combination was therefore used to sort cells from samples from this patient.

The diagnostic sample from patient 22005 showed only a relatively low fraction of cells with immature markers, but a relatively high fraction of leukemic cells showed a deficiency of CD13, which could be characterized as a leukemia-associated immunophenotype. This $CD33^+CD13^-$ population represented almost 29.09 % of the total live cell population in the diagnosis sample, this aberrant marker combination was therefore used for the planned sorts.

*Table 4.**Percentage of cells expressing surface markers of potential MRD cells observed in relation to live CD45+ cells obtained from MFC.** The patients identified as MRD positive from previous RT-qPCR were analyzed using MFC. The absolute number of cells for each patient expressing the phenotypes was compared to the absolute number of cells expressing CD45. The hierarchical gating strategy outlined in Figure 6 was applied.*

Sample ID	% $CD33^+CD34^+$	% $CD33^+CD13^-$	% $CD33^+CD56^+$	% $CD33^+CD117^+$	% $CD33^+CD7^+$	% $CD33^-CD13^+$
13156	A: 61.01 C: 1.18	A: 0.67 C: 1.20	A: 0.14 C: 0.65	A: 11.64 C: 1.10	A: 13.22 B: 3.26	A: 1.81 B: 0.81
22005	A: 1.33 B: 0.78	A: 29.09 B: 0.02	A: 15.90 B: 10.77	A: 14.47 B: 2.89	Not done	A: 0.83 B: 1.78
21029	B: 25.18 C: 1.26 D: 1.39 E: 1.66 F: 1.77	B: 8.53 C: 1.56 D: 1.31 E: 0.95 F: 0.53	B: 0.42 C: 7.03 D: 7.03 E: 2.43 F: 3.88	B: 42.01 C: 37.67 D: 1.43 E: 1.52 F: 1.42	B: 46.77 C: 14.97 D: 1.56 E: 1.17 F: 1.43	B: 1.95 C: 1.07 D: 2.48 E: 1.86 F: 3.26

3.3 Sorting of Cells with the Identified Immunophenotype from Diagnosis and Remission Samples from MRD Positive Patients.

Once we identified the phenotypes of interest for each patient, we then proceeded to sorting the cells based on the identified gating strategy (Table 5). As control populations, live cells and cells falling into the blast gate were sorted. For these control populations, a fixed number of cells were collected to facilitate the sorting of a maximum number of cells of specific phenotypes. Based on sample availability, sorting was done in duplicates or triplicates.

Patient 13156 was sorted (N=2) using the phenotypes $CD33^{+}CD34^{+}$. The average event number obtained was 522,839 from the diagnostic sample. From the remission sample, we sorted an average of 806 events of this phenotype.

Patient 21029 was sorted using $CD33^{+}CD117^{+}$ (N=3) with an average of 1,118,725 events collected from the diagnostic sample. The average Event number for this phenotype obtained for the remission sample (post-induction II) was 581 cells.

For the final patient, 22005, we acquired an average of 850,004 events at diagnosis, and an average of 561 events for the remission (post-induction) (N=2). The acquisition of live cells and blasts were set at a fixed number depending on the initial total cell count.

*Table 5. **Average of sorted cells indicated by events count on FACS**. The phenotypes sorted were selected based on previous flow cytometry. The live cells were determined by 7AAD staining. The blasts were identified using CD45 and side scatter after the selection of live cells. The phenotype gate was placed on the cells that were single, live blasts. The NOT phenotype indicates cells that do not fall into the phenotype gate. Diagnosis; D, Follow-up sample; FU. Data is represented as SD, displayed in parenthesis.*

Sample ID	Phenotype Sorted	Live	Blasts	Phenotype	NOT Phenotype
13156 (N=2)	$CD34^+$ $CD33^+$	D:50,000 FU:7,500	D:53,000 FU:5,000	D:522,839 FU:806	D:301,255 FU:256,973
21029 (N=3)	$CD117^+$ $CD33^+$	D: 10^5 FU:10,000	D: 10^5 FU:5,000	D:1,118,725 (+/- 449,747) FU:581.67 (+/- 384.31)	D:1,511,111 (+/- 183,847) FU: 8,895.33 (+/- 5,542)
22005 (N=2)	$CD13^-$ $CD33^+$	D: 10^5 FU: 10,000	D:10^5 FU:10,000	D: 850,004 FU:561	D:1,682,000 FU:290,667

3.4 Use of qPCR to Confirm Enrichment of Leukemic Cells in the Sorted Populations

The sorted samples were then subjected to qPCR analysis using previously established assays to determine the MRD level based on qPCR as a correlate of frequency of leukemic cells in the sample. The qPCR was performed for the specific subtype of NPM1 mutation found in the individual sample (Table 3). Results were normalized against endogenous control gene, ABL. All qPCRs were run with three technical replicates.

To illustrate the amount of target gene detected in the respective samples, live only cells of the diagnosis samples for all patients are shown along with live only, phenotype and NOT phenotype of the follow up samples. The goal of the sort was to enrich the leukemic cells in the sorted population as compared to the starting population (represented by the live population for the follow-up sample). Due to limitations in the amount of material available, samples from 2 of the 3 patients analyzed could only be sorted twice which limited possibilities for statistical analyses.

For patient 21029 the copy number of the target gene (NPM1 Type A) was on average 71,187 copies/10^4 ABL copies in the diagnosis (sorted for live cells), and 8,975 copies/

10^4 ABL copies for the follow-up. After sorting the follow-up sample for $CD33^+CD117^+$, the copy number of the target gene increased to 66,210 copies/10^4 ABL copies in the sorted populations, whereas it decreased to 1463 /10^4 ABL copies in the fraction of the blast gate that did not exhibit this specific immature progenitor phenotype (Figure 8). This shows that this progenitor sorting strategy for patient 21029 can facilitate an enrichment of leukemic cells to a level observed in the diagnostic sample.

For patient 22005 the copy number of the target gene (NPM1 Type D) was on average 83106 copies/10^4 ABL copies in the diagnostic sample, and 2497 copies /10^4 ABL copies in the follow up sample (sorted for viable cells). When sorted for cells of the most common phenotype in the leukemic sample ($CD33^+CD13^-$) this copy number of the target gene increased to 5305 copies/10^4 ABL copies in the sorted population of the follow-up, whereas it decreased 61 copies/10^4 ABL copies in the fraction of the blast gate that did not exhibit this specific immature progenitor phenotype (Figure 9). Interestingly, we also found on average a lower level of mutant NPM1 in the $CD33^+CD13^-$ fraction 52,573 copies /10^4 ABL copies compared to the control fraction within the blast gate, 83,105 copies /10^4 ABL copies. This heterogeneity of the expression of mutant NPM1 could therefore lead to an underestimation of the enrichment achieved and shows that the correlation of mutant NPM1 copies with the actual number of leukemic cells in the sample may not be perfect when analyzing subfractions of leukemic cells with different phenotypes.

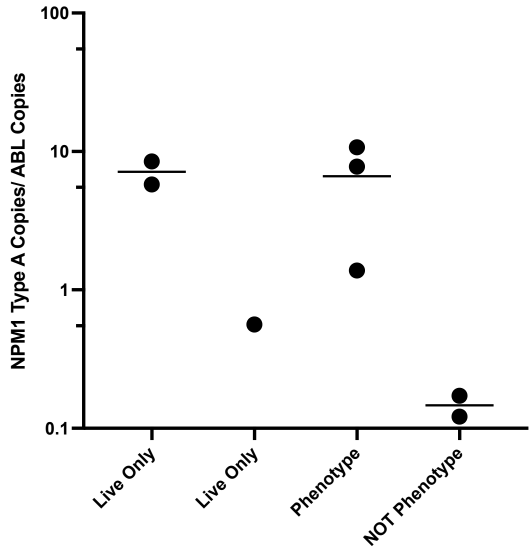

Figure 8. The qPCR results of the sorted cells from patient 21029, indicated by the standardized NPM1 Type A copies/ ABL copies. The live only dots on the left of the graph represent diagnosis sample. The second live only and onwards represent follow-up sample. Each dot represents a result of an individual sort. The qPCR was always completed in triplicates (n=3). Y axis in logarithmic scale. Mean of data presented (where N > 1). No units; transcript copy number

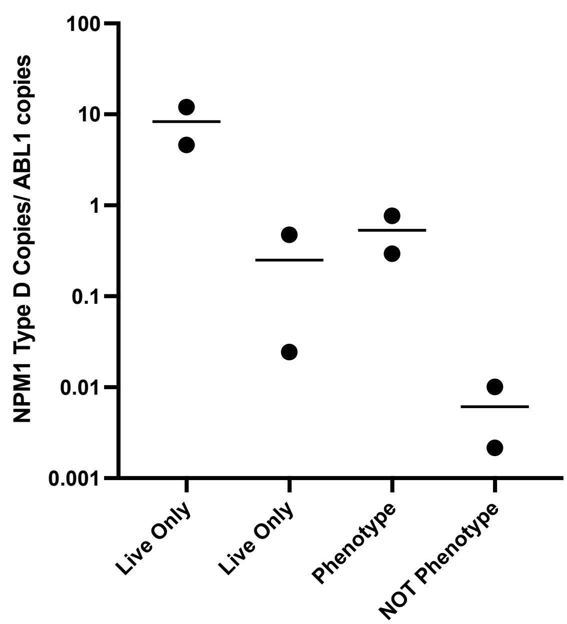

Figure 9. The qPCR results of the sorted cells from patient 22005 indicated by the standardized NPM1 Type D copies/ ABL1 copies. The live only on the far left is from sorted diagnosis sample. The second Live only column onwards is for follow-up sample. qPCR was always run-in triplicates (n=3). The y-axis is a logarithmic scale. Mean of data represented (where N > 1).

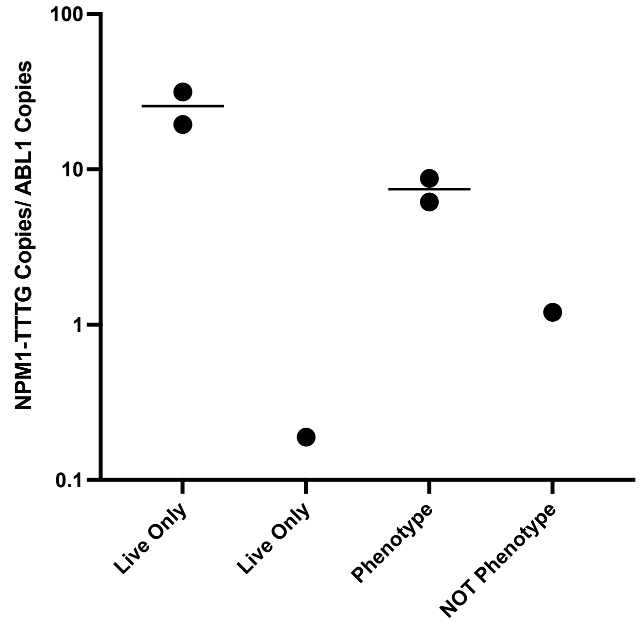

Figure 10. The qPCR results of the sorted cells from patient 13156, indicated by the standardized NPM1-TTTG copies/ 10^4 ABL copies. qPCR was run-in triplicates (n=3). The live only on the far left is from sorted diagnosis sample. The second Live only column onwards is for follow-up sample. The x-axis is a logarithmic scale. Mean of data represented (where N > 1).

For patient 13156, we found the target gene NPM1-TTTG was 255,355 copies/10^4 ABL copies in the diagnostic sample, and 1888 copies/10^4 ABL copies in the follow-up sample (both sorted for live cells). After sorting the follow-up sample for $CD33^+CD34^+$, the copy number of the target gene increased to 74631/10^4 copies ABL in the sorted population (Figure 10). The sort therefore led to an increase in the fraction of MRD cells in the sample that corresponds to approximately 30 % of diagnostic sample, which suggests that this progenitor sorting strategy may again be sufficient to sort MRD cells for molecular studies for this sample.

Chapter 4: Discussion

The goal of this project was the adaptation of clinical MRD strategies for the purpose of isolating MRD cells from remission samples. In the course of this work, we have made significant progress towards this goal. The approach required to first establish MRD assays in the lab and then to modify them to use these strategies for the enrichment of MRD cells. Molecular markers were used to identify suitable patient samples and to confirm the enrichment of MRD cells. We therefore had to focus our analysis on patient samples with relevant molecular MRD markers. This excluded many samples from the analysis. While we had longitudinal samples for 36 patients, only seven of them additionally had a molecular marker that we would follow using sensitive qPCR-based assays. This excluded many samples including high risk samples. While we could not use these samples for these pilot experiments, we will potentially be able to use them in the future as the established MFC panel can be used for >90% of patient samples.
For this project we adapted both a flow cytometric MRD panel as well as qPCR-based assay to detect four different types of mutant NPM1 as well as RUNX1-RUNX1T1 in our research laboratory. As these NPM1 qPCRs are designed to detect specific NPM1 mutations they usually do not fulfill criteria to apply the $\Delta\Delta$Ct method for relative quantification in qPCR and require standard curves. For two of the three NPM1 mutation subtypes commercial kits including standard curves were available, for one of the three NPM1 mutations a new standard had to be established. These quantitative PCR and the MFC panel are now available in the lab for future use.

The established molecular assays allowed to identify MRD positive follow up samples for three of the seven patients that could be investigated with these markers. As outlined above the molecular assays when applied to our samples and in this setting did often not fulfill criteria that would be required in a clinical laboratory workflow. Some of the reasons for this could include processing and storing times for the samples. In a clinical laboratory workflow, sample processing should usually happen within 24 hours of sample harvest. For us, most of the samples were processed within 72 hours which may have had an impact on viability and RNA integrity from these samples. The samples then also underwent mononuclear cell isolation and storing, which together with the cryo-recovery could impact sample integrity further. The negativity found for some of the samples could therefore also be due to a lack of established assay sensitivity. However, as the goal of this part of the project was to identify MRD positive patients this did not compromise our ability to setup sorting experiments.

There is even a more profound discrepancy between the flow cytometry processing for a clinical workflow and flow cytometry processing when using cryopreserved samples. In a clinical workflow, staining usually starts from unprocessed blood or marrow samples and follows a stain/ lyse/ wash protocol (Schuurhuis, et al., 2018). For optimum sensitivity most clinical flow cytometry laboratories do not perform mononuclear cell isolation before staining. Therefore, most of the staining protocols including the HARMONIZE panel used for our experiments also do not include a viability marker. This had to be adapted for our experiments where we integrated Live-Dead Red for the panel that we analyzed on the 5-laser Beckman Coulter Cytoflex instrument and 7AAD for the panel that we used for sorting. This inadvertently led to an omission of CD7 from the sorting panel, however as none of our samples had an aberrant expression of CD7 as optimal marker combination for sorting this again did not compromise our ability to design sorting experiments.

When analyzing the diagnostic samples for the three patients we were able to use in our sorting experiment we further found that if using a stringent MRD gating strategy, which would be useful in a clinical setting, we would presumably loose too many potential leukemic cells in the sorting and potentially select an non-representative subpopulation of leukemic cells from the follow-up samples. So, while the HARMONIZE consortium uses gating on specific myeloid progenitor markers in combination with aberrant marker expression (Rohnert M, 2020), we looked at aberrant marker and progenitor marker combinations separately and defined a less stringent approach for sorting. In our case, patient 13156 presented $CD33^+CD34^+$, patient 22005 presented $CD13^-CD33^+$, and patient 21029 presented $CD33^+CD117^+$ markers. While the combinations $CD33^+CD34^+$ and $CD33^+CD117^+$ can also be found on normal myeloid progenitors, these marker combinations still proved useful for enriching MRD cells as demonstrated by qPCR.

To our surprise, we found differences in the level of mutant NPM1 detected in the different sorted subpopulation for sample 22005, wherein asynchronous expression of CD33 and CD13 was used to identify leukemic cells. This heterogeneity in the detection of mutant NPM1 could be a result of clonal differences between the presence of the mutation or more likely expression differences in NPM1 between the different subpopulations. This interesting finding could result in problems when estimating the frequency of leukemic cells based on the qPCR for mutant NPM1 as the correlation between mutant NPM1 copies with the frequency of leukemic cells in the sample is then not perfect. This finding would also need to be taken into consideration when planning comparative expression studies. These would then only be valid if both compared populations have undergone the same processing.

The most important limitation of our work at the moment is the low number of sorted events that we obtained when applying our sorting strategy. These were usually below 1000 cells for each sorting experiment. This would make our strategy currently not applicable for functional or molecular experiments using sophisticated assays such as single-cell RNA sequencing.

While the low number of cells obtained is obviously in part a consequence of the low frequency of the phenotype of interest in the sample, additional factors such as sample size and viability are certainly also contributing. Future experiments for the three patients evaluated in this thesis could maximize the number of cells obtained by only sorting out the cell population of interest (phenotypes), since in the preceding sorting experiments we also sorted control populations. Additional follow up samples for these patients are also available, in particular for patient 21029 where some of the follow up sample show a higher MRD level. However, if these optimization steps do not result in an improvement in the yield of cells obtained from the sorting, additional modifications of the protocol such as a more stringent sample processing timeline or even the use of fresh samples have to be considered.

While we know that we can sort out living cells from these cryopreserved samples based on the staining with 7AAD, these may still be compromised already and not be sufficiently viable to read out in functional assays. As the qPCRs also shows that the RNA yield and the level of ABL measured in the samples showed a great variability, this could again compromise the ability to use these sorted cells for sensitive applications such as single-cell RNA sequencing. In summary, while a significant progress was made in our ability to sort MRD cells from remission samples, additional optimization steps are required, in particular if the obtained cells will be used in sensitive applications.

Conclusion

In summary, we have made significant progress in our ability to enrich MRD cells from remission samples from AML patients. Many new methods had to be pioneered in this process including an MFC panel designed for clinical MRD detection as well as several qPCR assays to detect MRD cells. Similar methods are currently moving into clinical labs and will improve the treatment of patients with AML. In my work, I was confronted with some of the challenges when establishing these methods in a research lab. We have also made progress with enriching MRD cells by flow cytometric sorting. While there are still technical challenges that will need to be overcome, this method could aid future research to understand the biology of MRD cells. This better understanding of the biology of MRD may help us develop new treatment strategies for this disease to reduce the risk of relapse in AML patients.

Bibliography

Almeidaa, A., & Fernando, R. (2016). Acute myeloid leukemia in the older adults. *Leukemia Research Report*, 1-7.

Alpermann, T., Schnittger, S., Eder, C., Dicker, F., Meggendorfer, M., Kern, W., . . . Staib, P. (2016). Molecular subtypes of NPM1 mutations have different clinical profiles, specific patterns of accompanying molecular mutations and varying outcomes in intermediate risk acute myeloid leukemia. *Haematologica*, 55-58.

American Cancer Society. (2018). *Acute Myeloid Leukemia (AML) Subtypes and Prognostic Factors*. Retrieved from Cancer.org: https://www.cancer.org/cancer/acute-myeloid-leukemia/detection-diagnosis-staging/how-classified.html#written_by

Arber, D. A., Orazi, A., Hasserjian, R., Thiele, J., Borowitz, M., Le Beau, M., . . . Vardiman, J. (2019). The 2016 revision to the World Health Organization classification of myeloid neoplasms and acute leukemia. *Blood*, 2391–2405.

Bhat S., R. F. (2019). CD117: Lineage assigning marker in acute myeloid leukemias. *International Journal of Advances in Medicine*, 382-388.

Bonnet D, D. J. (1997). Human acute myeloid leukemia is organized as a hierarchy that originates from a primitive hematopoietic cell. *Nature Med.*, 730-737.

Boyd, A., Aslostovar, L., Reid, J., Leber, B., Bhatia, M., & Xenocostas, A. (2018). Identification of Chemotherapy-Induced LeukemicRegenerating Cells Reveals a Transient Vulnerability of Human AML Recurrence. *Cancer Cell*(34), 483–498.

Breitman, T., Collins, A., & Keene, B. (1981). Terminal differentiation of human promyelocytic leukemic cells in primary culture in response to retinoic acid. *Blood, 57*(6), 1000-1004.

Buccisano F, M. L. (2012). Prognostic and therapeutic implications of minimal residual disease detection in acute myeloid leukemia. *Blood*, 332-341.

Cheson BD, B. J. (2003). Revised recommendations of the International Working Group for Diagnosis, Standardization of Response Criteria, Treatment Outcomes, and Reporting Standards for Therapeutic Trials in Acute Myeloid Leukemia. *J Clin Oncol.*, 4642-9.

Christopher MJ, P. A. (2018). Immune Escape of Relapsed AML Cells after Allogeneic Transplantation. *New England J Medicine*, 2330-2341.

Colombo E, M. J. (2002). Nucleophosmin regulates the stability and transcriptional activity of p53. *Nature Cell Biology*, 529-533.

Daver, N., Schlenk, R., Levis, M., & Russel, N. (2019). Targeting FLT3 mutations in AML: review of current knowledge and evidence. *Leukemia*(33), 299-312.

Devine, S., Owzar, K., Blum, W., Mulkey, F., Stone , R., Hsu, J., . . . Vij, R. (2015). Phase II Study of Allogeneic Transplantation for Older Patients With Acute Myeloid Leukemia in First Complete Remission Using a Reduced-Intensity Conditioning Regimen. *J Clin Oncol, 33*(35), 4167-4175.

DiNardo CD, J. B. (2020). Azacitidine and venetoclax in previoulsy untreated acute myeloid leukemia. *New england journal of medicine*, 617-629.

Dohner, H., Estey, E., Grimwade, D., Amadori, S., Appelbaum, F., Buchner, T., . . . Levine, R. (2017). Diagnosis and management of AML in adults: 2017 ELN recommendations from an international expert panel. *Blood, 129*(4), 424–447.

Dombret, H., Seymour, J., Aleksandra, B., Wierzbowska, A., Jang, J., & Kumar, R. (2015). International phase 3 study of azacitidine vs conventional care regimens in older patients with newly diagnosed AML with >30% blasts. *Blood, 126*(3), 291-299.

Estey, E., & Dohner, H. (2006). Acute myeloid leukaemia. *The Lancet*, 1894-1907.

Facts and Statistics: Blood Cancer. (2016). Retrieved from Leukemia and Lymphoma Society of Canada: https://www.llscanada.org/disease-information/facts-and-statistics

Falini, B., Bolli, N., Shan, J., Martelli, M., Liso, A., Pucciarini, A., & Bigernea, B. (2006). Both carboxy-terminus NES motif and mutated tryptophan(s) are crucial for aberrant nuclear export of nucleophosmin leukemic mutants in NPMc+ AML. *Blood*, 4514-4523 .

Falini, B., Mecucci, C., Tiacci, E., Alcalay, M., Rosati, R., Pasqualucci, L., . . . Colombo, E. (2005). Cytoplasmic Nucleophosmin in Acute Myelogenous Leukemia with a Normal Karyotype. *N Engl J Med*, 254-266.

Foster, C. T., Dovey, O. M., Lezine, L., Luo, J. L., Gant, T. W., Barlev, N., . . . Cowley, S. M. (2010). Lysine-Specific Demethylase 1 Regulates the Embryonic Transcriptome and CoREST Stability. *Mol Cell Biol*(30), 4851-4863.

Freeman SD, H. R. (2018). MEasurable residual disease at induction redefines partial response in acute myeloid lekemia and stratifies outcomes in patients at stratifies outcomes in patients at standard risk without NPM1 mutation. *Clinical oncology*, 1486-1497.

Gilliland DG., G. J. (2002). The roles of FLT3 in hematopoiesis and leukemia. *Blood, 100*(5), 1532-1542.

Gilliland, D., & Tallman, M. (2002). Focus on Acute Leukemias. *Cancer Cell*, 417-420.

Harrington A, O. H. (2012). A Dissection of the CD45/Side Scatter “Blast Gate” . *American journal of clinical pathology*, 800-804.

Heuser M., F. S. (2021). 2021 Update on MRD in acute myeloid leukemia: a consensus document from the European LeukemiaNet MRD Working Party. *Blood*, 138 (26): 2753–2767.

Ho, T., LaMere, M., Stevens, B., Ashton, J., Myers, J., O'Dwyer, K., & Liseveld, J. (2016). Evolution of acute myelogenous leukemia stem cell properties after treatment and progression. *Blood, 128*(13), 1671–1678.

Huang, J., Sengupta, R., Espejo, A., Lee, M., Dorsey, J., Richter, M., . . . Bedford, M. (n.d.). p53 is regulated by the lysine demethylase LSD1. *Nature, 2007*(449), 105-108.

Hui G, L. A. (2020). 1034 Routine Use of Gemtuzumab Ozogamicin in 7+3-Based Inductions for All “Non-Adverse” Risk AML. *ASH Annual meeting and Exposition*.

Ivey, A., Hills, R., Simpson, M., Jovanovic, J., Gilkes, A., Grech, A., & Patel, Y. (2016). Assessment of Minimal Residual Disease in Standard-Risk AML. *N Engl J Med*, 22-433.

Jaiswal S, E. B. (2019). Clonal hematopoiesis in human aging and disease. *Science*, 366(6465).

Kohnke T, B. V.-T. (2019). Response assessment in acute myeloid leukemia by flow cytometry supersedes cytomorphology at time of aplasia, amends cases without molecular residual disease marker and serves as an independent prognostic marker at time of aplasia and post-induction. *Haematologica*.

Krönke J, S. R. (2011). Monitoring of Minimal Residual Disease in NPM1-Mutated Acute Myeloid Leukemia: A Study From the German-Austrian Acute Myeloid Leukemia Study Group. *Journal of clinical oncology*.

Kronke, J., Bullinger, L., Teleanu, V., Tschürtz, F., Kuhn, M., Gaidzik, V., . . . Paschka, P. (2013). Clonal evolution in relapsed NPM1-mutated acute myeloid leukemia. *Blood*, 100-108.

Krupka C, K. P. (2014). CD33 target validation and sustained depletion of AML blasts in long-term cultures by bispecific T-cell-engaging antibody AMG330. *Blood*, 356-365.

Löwenberg B., P. T. (2011). Cytarabine Dose for Acute Myeloid Leukemia. *N Engl J Med., 364*, 1027-1036.

Lacombe F, C. L. (2018). Prognostic value of multicenter flow cytometry harmonized assessment of minimal residual disease in acute myeloblastic leukemia. *Hematological Oncology*, 422-428.

Lapidot T, S. C.-C. (1994). A cell initiating human acute myeloid leukaemia after transplantation into SCID mice. *Nature*, 367(6464):645-8.

Lee-Six H, O. N. (2018). Population dynamics of normal human blood inferred from somatic mutations. *Nature*, 473-478.

leukemia statistics. (2020, February 28). Retrieved from canadian cancer society: https://www.cancer.ca/en/cancer-information/cancer-type/leukemia/statistics/?region=bc

Ley, T. J., Ding, L., Walter, M., & McLellan, M. D. (2010). DNMT3A Mutations in Acute Myeloid Leukemia. *N. Engl. J. Med.*(363), 2424-2433.

Lovell, A. (2019). Midostaurin (Rydapt®). *Oncology Times*, *41*(24), 5.

Ludwig W., S. K. ((2000)). How quantitative is quantitative PCR with respect to cell counts? *Systematic and Applied Microbiology*, 23, 556-562.

Martens JHA., S. H. (2010, June 18). The molecular signature of oncofusion proteins in acute myeloid leukemia. *FEBS Lett*, *584*(12), 2662-2669.

Mencia-Trinchant N. (2017). Minimal Residual Disease Monitoring of Acute Myeloid Leukemia by Massively Multiplex Digital PCR in Patients with NPM1 Mutations. *Journal of Molecular Diagnostics*,.

Mitelman F, J. B. (2007). The impact of translocations and gene fusions on cancer causation. *Nat Rev Cancer*, *7*(4), 233-245.

Muffly , L., Pasquini, M., Martens, M., Brazauskas , R., Zhu, X., Adekola, K., . . . Ballen, K. (2017). Increasing use of allogeneic hematopoietic cell transplantation in patients aged 70 years and older in the united states. *Blood*(130), 1156–1164.

Munshi, N., Avet-Loisseau, H., Rawstron, A., Owen, R., Child, A., Thakurta, A., . . . Georgieva, A. (2018). Minimal residual disease predicts superior survival in patients with multiple myeloma: a meta-analysis. *JAMA Oncol*, 28-35.

Ng S, M. A. (2016). A 17-gene stemness score for rapid determination of risk in acute leukaemia. *Nature*, 433-437.

Ostronoff, F., Othus, M., Lazenby, M., Estey, E., Appelbaum, F., Evans, A., . . . Kopecky, K. (2015). Prognostic significance of NPM1 mutations in the absence of FLT3-internal tandem duplication in older patients with acute myeloid leukemia: a SWOG and UK National Cancer Research Institute/Medical Research Council report. *J. Clin Oncol.*, 1157-1164.

Papaemmanuil, E., Gerstung, M., Bullinger, L., Gaidzik, V., Paschka, P., & Roberts, N. (2016). Genomic Classification and Prognosis in Acute Myeloid Leukemia. *N Eng J Med, 374*(23), 2209-2221.

Raphael BJ, M. A. (2013). Genomic and epigenomic landscapes of adult de novo acute myeloid leukemia. *New England Journal of Medicine*, 2059-2074.

Rohnert M, v. B. (2020). Standardized identification of measurable residual disease (MRD) by multicolor flow cytometry (MFC) in patients with acute myeloid leukemia (AML). *European Hematology Association*, EP566.

San Miguel, J., Vidriales, M., Lopez-Berges, C., Diaz-Mediavilla, J., Gutierrez, N., Canizo, C., & Fernando, R. (2001). Early immunophenotypical evaluation of minimal residual disease in acute myeloid leukemia identifies different patient risk groups and may contribute to postinduction treatment stratification. *Blood, 98*(6), 1746–1751.

Schuurhuis, G. J., Heuser, M., Freeman, S., B'en'e, M.-C., Buccisano, F., Cloos, J., . . . Hills, R. K. (2018). Minimal/measurable residual disease in AML: a consensus document from the European LeukemiaNet MRD Working Party. *Blood, 131*(12), 1275-1291.

Shi, Y., Lan, F., Matson, C., Mulligan, P., Whetstine, J., Cole, P., & et, a. (2004). Histone demethylation mediated by the nuclear amine oxidase homolog LSD1. *Cell*(119), 941-953.

Shlush LI, Z. S. (2014). Identification of pre-leukaemic haematopoietic stem cells in acute leukaemia. *Nature*, 328-333.

Siegel RL, M. K. (2022). Cancer statistics, 2022. *American Cancer Society*.

Suzuki, T., Kiyoi, H., Ozeki, K., Tomita, A., Yamaji , S., Suzuki, R., . . . Miyawaki, S. (2005). Clinical characteristics and prognostic implications of NPM1 mutations in acute myeloid leukemia. *Blood*, *106*, 2854-2861 .

ThermoFisher. (2003). *Creating Standard Curves with Genomic DNA or Plasmid DNA Templates for Use in Quantitative PCR.* Retrieved from Applied Biosystems.

Thol F., G. R. (2018). Measurable residual disease monitoring by NGS before allogeneic hematopoietic cell transplantation in AML. *Blood*, 132(16):1703-1713.

Thomas D, M. R. (2017). Biology and relevance of human acute myeloid leukemia stem cells. *Blood*, 1577-1585.
Thomas, M. L. (1989). The Leukocyte Common Antigen Family. *Ann. Rev. Immunol.*(7), 339-369.
Tilly, H., Castaigne, S., Bordessoule, D., Casassus , P., Le Prise, P., & Tertian, G. (1990). Low-dose cytarabine versus intensive chemotherapy in the treatment of acute nonlymphocytic leukemia in the elderly. *J. Clin. Oncol.*, *8*(2), 272–279.
Ustun, C., Lazarus, H., & Weisdorf, D. (2013). To transplant or not: a dilemma for treatment of elderly AML patients in the twenty-first century. *Bone Marrow Transplant*, *48*(12), 1497-1505.
Watts, J. M., Bradley, T. J., Thomassen, A., Trang-Dinh, Y., & Tejera, D. (2018). The Lysine-Specific Demethylase 1 (LSD1) Inhibitor Tranylcypromine (TCP) in Combination with ATRA Is Tolerable and Has Anti-Leukemic Activity in Adult Patients with Relapsed/Refractory AML and MDS. *Blood*(132), 2721.
Welch JS, L. T. (2012). The Origin and Evolution of Mutations in Acute Myeloid Leukemia. *Cell*, 264-278.
Whyte, W. A., Bilodeau, S., Orlando, D. A., Hoke, H. A., Frampton, G. M., & Foster, C. T. (2012). Enhancer decommissioning by LSD1 during embryonic stem cell differentiation. *Nature*(482), 221-225.
Wissmann, M., Yin, N., Muller, J., Greschik, H., Fodor, B., & Jenuwein, T. (2007). Cooperative demethylation by JMJD2C and LSD1 promotes androgen receptor-dependent gene expression. *Nat Cell Biol*(9), 347-353.
Wong HY, S. A. (2019). Molecular Measurable Residual Disease Testing of Blood During AML Cytotoxic Therapy for Early Prediction of Clinical Response. *Frontiers in Oncology*.

Appendix

Appendices A.

Where available, clinical quantitative PCR reagents were used. As these reagents are usually used for samples with non-limiting cell numbers, we evaluated the minimum number of cells that could be detected in these assays using cell lines (See Appendix A Table 1). Varying amounts of OCI-AML3 with HL-60 were used to assess the sensitivity of the qPCR test (see Appendix A for qPCR sensitivity tests). Standard curves were analyzed to identify the line equation (See Appendix A, Fig. 1). The line equation was used to find the copy number for NPM1 mutations in each sample. The copy numbers obtained from the equation for each concentration was standardized with the ABL control. The average was utilized in identifying the copy number from the respective equations. Following the calculations for copy number, the data was normalized by dividing the NPM1-mutation results with ABL-control of the samples.
The cell lines used for experiments with the aim of optimization are presented with specified characteristics. The cell lines were used in qPCR, and multiparameter flow cytometery optimization steps.
The qPCR test for sensitivity optimized to identify the minimum cell number required for future experiments; the sorted cells from the fluorescence-activated cell sorter. The minimum detectable cells identified in the test is 1000 cells, indicated by the average cycle threshold value of the OCI-AML3 cell line.

Table 6. Cell lines used for optimization experiments.

Cell Line	***Obtained from***	***Characteristic***
OCI-AML3	DSMZ	NPM1 Type A mutation
HL-60	ATCC	Promyelocytic; M2-M6

Table 7. The qPCR results of different cell lines used for the identification. The cell line OCI AML 3 was identified as an NPM1 mutated cell line, while HL60 is a promyelocytic cell line without the NPM1 mutation. The average cycle threshold number is indicated, with the copy number. The standardized transcript copy number is also presented (NPM1/ABL).

Cell line Ratio	Average Ct	log Copy number	Copy number	NPM1/ABL
1000:1000	29.04	3.37	2329.28	7.00
10000:10000	26.60	4.08	12016.68	6.89
1000 OCI	27.92	3.69	4941.03	18.32
10000 OCI	25.68	4.35	22308.96	12.27
1000 HL60	0	N/A		
10000 HL60	0			

Appendix B.

The development of the standard for patient 13156 is still ongoing as final optimizations are required. The development of the standards is highlighted in this section.

Table 8. The PCR program used to increase the amount of NPM1-TTTG mutation.

PCR program steps	Temperature (ºC)	Time
Initial Denaturation	94	1 minute
Denature	94	15 seconds
Anneal	53.5	30 seconds
Extend	68	1 minute
Hold	4	10 minutes

Table 9. The primers used for the development of the NPM1-TTTG mutation.

Primer	***Sequence***	***Concentration used***
TTTG primer Forward	5'- GAAGAATTGCTTCCGGATGACT-3'	200 nM
TTTG primer Reverse	5'- TCCTCCACTGCCAAACAGA-3'	200 nM
M13 Forward	5´-GTAAAACGACGGCCAG-3´	1 µM
M13 Reverse	5´-CAGGAAACAGCTATGAC-3´	1 µM

Table 10. The development of the standards for patient 13156 (NPM1-TTTG). The final concentration was identified by dividing the mass of the plasmid DNA by 5 uL.

Copy number	Plasmid size (grams)	Mass of Plasmid DNA (grams)	Final plasmid concentration (g/ul)
1 million	x 0.394e-17	0.394e-11	7.88e-13
100, 000		0.394e-12	7.88e-14
10, 000		0.394e-13	7.88e-15
1000		0.394e-14	7.88e-16
100		0.394e-15	7.88e-17
10		0.394e-16	7.88e-18

Table 11.The final copy numbers were determined by serial dilution using the final concentration of the 1 million copy number.

Tube	Source of Plasmid	Volume of Plasmid	Volume of Diluent (NFW)	Final Volume	Final concentration (g/uL)	Copy number
1	Stock	10	990	1000	$2x\ 10^{-8}$	N/A
2	1	10	990	1000	$2x\ 10^{-10}$	
3	2	10	990	1000	$2x10^{-12}$	
4	3	39.4	60.6	100	7.88e-13	1 million
5	4	10	90	100	7.88e-14	100,000
6	5	10	90	100	7.88e-15	10,000
7	6	10	90	100	7.88e-16	1000
8	7	10	90	100	7.88e-17	100
9	8	10	90	100	7.88e-18	10

Figure 11. ***Graphs illustrate the quantification of the standards, as well as the corresponding line equation.*** *Graph A corresponds to the NPM1 standard. Graph B corresponds to the ABL standard. Finally, graph C corresponds to the NPM1-TTTG standard. SD used, with n=3.*